

**Manuscript version: Author's Accepted Manuscript**

The version presented in WRAP is the author's accepted manuscript and may differ from the published version or Version of Record.

**Persistent WRAP URL:**

<http://wrap.warwick.ac.uk/162646>

**How to cite:**

Please refer to published version for the most recent bibliographic citation information. If a published version is known of, the repository item page linked to above, will contain details on accessing it.

**Copyright and reuse:**

The Warwick Research Archive Portal (WRAP) makes this work by researchers of the University of Warwick available open access under the following conditions.

© 2022 Elsevier. Licensed under the Creative Commons Attribution-NonCommercial-NoDerivatives 4.0 International <http://creativecommons.org/licenses/by-nc-nd/4.0/>.



**Publisher's statement:**

Please refer to the repository item page, publisher's statement section, for further information.

For more information, please contact the WRAP Team at: [wrap@warwick.ac.uk](mailto:wrap@warwick.ac.uk).

1 **A Review on Chemometric Techniques with Infrared, Raman and Laser-induced**  
2 **Breakdown Spectroscopy for Sorting Plastic Waste in the Recycling Industry**

3 **Authors** Edward Ren Kai Neo<sup>a,b\*</sup>, Zhiquan Yeo<sup>b</sup>, Jonathan Sze Choong Low<sup>b</sup>, Vanessa  
4 Goodship<sup>a</sup>, Kurt Debattista<sup>a</sup>

5 <sup>a</sup>*Warwick Manufacturing Group, University of Warwick, Coventry, CV4 7AL, United Kingdom*

6 <sup>b</sup>*Singapore Institute of Manufacturing Technology, 2 Fusionopolis Way, Singapore 138634,*  
7 *Singapore*

8 *\*Corresponding author: edward.neo@warwick.ac.uk (Email)*

9 **Abstract**

10 Mismanagement of plastic waste globally has resulted in a multitude of environmental issues,  
11 which could be tackled by boosting plastic recycling rates. Chemometrics has emerged as a  
12 useful tool for boosting plastic recycling rates by automating the plastic sorting and recycling  
13 process. This paper will comprehensively review the recent works applying chemometric  
14 methods to plastic waste sorting. The review begins by introducing spectroscopic methods and  
15 chemometric tools that are commonly used in the plastic chemometrics literature. The  
16 spectroscopic methods include near-infrared spectroscopy (NIR), mid-infrared spectroscopy  
17 (MIR), Raman spectroscopy and laser-induced breakdown spectroscopy (LIBS). The  
18 chemometric tools include principal component analysis (PCA), linear discriminant analysis  
19 (LDA), partial least square (PLS), k-nearest neighbors (k-NN), support vector machines (SVM),  
20 random forests (RF), artificial neural networks (ANNs), convolutional neural networks (CNNs)  
21 and K-means clustering. This review revealed four main findings. 1) The scope of plastic waste  
22 should be expanded in terms of types, contamination and degradation level to mirror the  
23 heterogeneous plastic waste received at recycling plants towards understanding potential  
24 application in the recycling industry. 2) The use of hybrid spectroscopic method could  
25 potentially overcome the limitations of each spectroscopic methods. 3) Develop an open-  
26 sourced standardized database of plastic waste spectra would help to further expand the field.  
27 4) There is limited use of more novel machine learning tools such as deep learning for plastic  
28 sorting.

29 **Keywords:** Chemometrics; spectroscopy; hyperspectral imaging; spectral analysis; machine  
30 learning; plastic recycling

31 **Abbreviations**

32 ABS - Acrylonitrile Butadiene Styrene

33 HDPE – High Density Polyethylene

34 HSI - Hyperspectral Imaging

35 IR - Infrared

36 LDPE – Low Density Polyethylene

37 LLDPE – Linear Low Density Polyethylene

38 LIBS – Laser-induced Breakdown Spectroscopy

39 MIR – Mid Infrared

40 NIR – Near Infrared

41 PA - Polyamide

42 PC - Polycarbonate

43 PE - Polyethylene

44 PLA – Polylactic Acid

45 PMMA – Polymethyl Methacrylate

46 POM - Polyoxymethylene

47 PP – Polypropylene

48 PS - Polystyrene

49 PTFE - Polytetrafluoroethylene

50 PU - Polyurethane

51 PVC – Polyvinyl Chloride

52

53

54

55

56

57

58

59

60

## 61 **1. Introduction**

62 Plastic is a versatile material used for a wide range of applications, such as packaging,  
63 construction and agriculture. The demand for plastics has increased 200-fold over the past 70  
64 years, with 381 million tons of plastics produced annually in 2015 and over 8 billion tons of  
65 total production produced to date (Geyer et al., 2017; Ritchie, 2018). Managing the resulting  
66 increase in plastics waste generated has become an increasingly critical global challenge. It has  
67 been estimated that only 9% of all the plastics ever generated have been recycled, while the  
68 vast majority were landfilled (Geyer et al., 2017).

69 Due to the mismanagement of plastic waste, a large amount of plastic waste has leaked into the  
70 oceans; this has been linked to a multitude of environmental issues (Jambeck et al., 2015).  
71 Plastic is known to be extremely persistent in the environment and could disrupt the marine  
72 ecosystem through pathways such as ingestion or entanglement (Ferronato and Torretta, 2019).  
73 Microplastics also accumulate in the food chain and were recently found in human placenta  
74 (Ragusa et al., 2021), which could potentially be linked to harmful effects for humans  
75 (Campanale et al., 2020). At the current rate of plastic waste management, it is projected that  
76 the weight of plastics in the ocean would exceed that of fish by 2050 (Ellen MacArthur  
77 Foundation, 2017), highlighting the severity and urgency of addressing plastic pollution, which  
78 could be addressed by boosting plastic recycling.

79 While plastic recycling rates have generally been trending upwards over the years, plastic  
80 recycling rates remain low globally at around 18% (OECD, 2018). The factors contributing to  
81 low recycling rate for plastics has been well studied, and includes various economic,  
82 information, technical and legislation barriers (Hopewell et al., 2009; Milios et al., 2018;  
83 Suchismita, 2017; Tesfaye and Kitaw, 2020). Proper sorting of plastic waste is one way to  
84 overcome some of the barriers. Plastic sorting has traditionally relied on a combination of  
85 manual labor and physical methods (Dodbiba and Fujita, 2004). These traditional methods  
86 utilize physical properties of plastic for sorting, such as density and electrical conductivity.  
87 More detailed reviews of these traditional methods have previously been conducted and will  
88 be out of scope of this paper (Al-Salem et al., 2009; Gundupalli et al., 2017; Malcolm Richard  
89 et al., 2011; Wang et al., 2015; Wu et al., 2013).

90 One drawback of physical methods is the lack of a feedback mechanism to constantly monitor  
91 the quality of plastic waste going into recycling, limiting the traceability of plastic type and  
92 quality for recycling. In recent times, solutions focusing on automated plastic sorting systems

93 with machine learning techniques are on the rise. Some systems have approached it as an image  
94 recognition task, which is useful for identifying common plastic products like mineral water  
95 bottles (Wang et al., 2019). Other systems have explored using chemometrics, which involves  
96 the use of chemical data from spectroscopy methods (Heberger, 2008) for automatic sorting of  
97 plastic waste. Chemometrics have been widely applied towards quality control in the food  
98 (Liang et al., 2020) and pharmaceutical industries (Biancolillo and Marini, 2018),  
99 environmental modelling (Chapman et al., 2020) and forensics (Sauzier et al., 2021), but  
100 chemometric techniques have only recently gained popularity in the area of plastic waste (da  
101 Silva and Wiebeck, 2020). A broad review of various physical and chemometric-based method  
102 for municipal solid waste sorting was performed recently (Gundupalli et al., 2017). Other  
103 reviews have studied the use of chemometrics for microplastics detection with Raman (Araujo  
104 et al., 2018) and Fourier transform infrared (FTIR) spectroscopy (Veerasingam et al., 2020),  
105 but none, so far, have focused on plastic waste sorting.

106 This work aims to build upon the literature by comprehensively reviewing the use of  
107 chemometric method specifically for plastic waste sorting, and assessing the state of the field  
108 for application in the recycling industry. This would contribute towards helping to determine  
109 the research directions that can be undertaken to help develop a state-of-the-art plastic sorting  
110 approach which can effectively sort out recyclable polymers from post-consumer plastic waste.  
111 The surveyed literature was found using the search terms ‘plastic’, ‘recycling’ and  
112 ‘chemometrics’ or one of the spectroscopic method ‘Infrared’, ‘Raman’, ‘LIBS’ on Scopus,  
113 Web of Science and Google Scholar. Section 2 will provide a background on spectroscopic  
114 methods that can be used to obtain chemical data of plastics, and chemometric techniques to  
115 analyze the chemical data; section 3 will cover methodology applied for the literature review;  
116 sections 4 to 6 will cover specific works that have been done in this field using infrared, Raman  
117 and LIBS data respectively; section 7 will discuss and evaluate the limitations and gaps in using  
118 spectroscopic data for chemometric analysis.

119

120

121

122

123

## 124 **2. Background**

125 This section will first introduce some spectroscopic methods that have been widely used to  
126 obtain chemical data from plastic in a non-destructive manner. Following that, chemometric  
127 techniques that are widely used to analyze spectroscopic data of plastics will be introduced.

### 128 **2.1 Spectroscopic Methods**

129 Spectroscopy is the study of interaction between electromagnetic radiation and matter. There  
130 are broadly three types of spectroscopic methods that are commonly used for chemometrics  
131 sorting of plastic, which are infrared spectroscopy, Raman spectroscopy and laser-induced  
132 breakdown spectroscopy, which will be described in this section. A comparison of the three  
133 spectroscopic methods will be further presented in section 7.

#### 134 **2.1.1 Infrared Spectroscopy**

135 Infrared (IR) spectroscopy measures the absorption or reflectance of IR radiation by chemicals  
136 or materials (Griffiths et al., 2007). The electromagnetic radiation in this region is typically  
137 associated with the rotational and vibrational frequencies of different chemical bonds within  
138 the molecules. These are termed resonant frequencies, which are absorbed by the molecules,  
139 while the other frequencies would be transmitted. Fourier transform infrared spectroscopy  
140 (FTIR) applies a mathematical technique known as Fourier transform to convert the raw time  
141 domain signals into an easily visualizable IR spectrum (Griffiths et al., 2007), which maps the  
142 IR radiation absorbed/transmitted over each frequency, thus generating a molecular fingerprint.  
143 The IR region is further divided into far-, mid- and near-IR, each containing different  
144 information. Rotational frequencies can be found within far-IR, while fundamental vibrational  
145 frequencies can be found within mid-IR and overtones of vibrational frequencies can be found  
146 within near-IR (Veerasingam et al., 2020).

#### 147 **2.1.2 Raman Spectroscopy**

148 Raman spectroscopy is another technique used to study the rotational and vibrational  
149 frequencies of chemical bonds within a molecule (McCreery, 2005). When photons from a  
150 laser interact with the molecular vibrations, molecules can be excited to a higher energy level.  
151 Most of this energy will be dissipated through elastic scattering (or Rayleigh scattering), where  
152 the energy of the emitted photons is equal to the photon from the laser. Raman spectroscopy  
153 measures the wavelength of inelastically scattered photons, where the emitted photon is higher  
154 or lower in energy as compared to the photon from the laser, which can be visualized in a

155 spectrum of intensity over wavelength. As the majority of scattered photons are elastically  
156 scattered, a light filter is often used to filter out the scattered radiation to allow better  
157 observation of the inelastically scattered photons.

### 158 **2.1.3 Laser-induced Breakdown Spectroscopy**

159 Laser-induced breakdown spectroscopy (LIBS) is an elemental analysis technique that can be  
160 used to detect the presence of all elements (Singh and Thakur, 2020). It focuses a high energy  
161 laser on a sample to vaporize and atomize a small amount of material into plasma.  
162 Characteristic radiation emitted by each of the element can be detected to confirm the presence  
163 of different elements.

## 164 **2.2 Chemometric Techniques**

165 The chemical data obtained via spectroscopic methods can be analyzed with various  
166 chemometric tools. While there are significant numbers of possible tools, this work will focus  
167 on the ones used in the chemometrics publications. A broad category of tools frequently used  
168 in chemometrics research are dimensionality reduction tools such as principal component  
169 analysis (PCA), linear discrimination analysis (LDA) and partial least squares regression (PLS).  
170 Supervised machine learning, where labelled data is used to train the model to classify the  
171 plastic from the spectrum obtained using spectroscopic methods, can also be used. These  
172 include tools like k-nearest neighbor (k-NN), support vector machines (SVM), random forest  
173 and neural networks. Limited works also explored unsupervised machine learning in the form  
174 of k-means clustering.

### 175 **2.2.1 Principal Component Analysis**

176 PCA is a dimensionality reduction tool used for multi-dimensional datasets (Jolliffe and  
177 Cadima, 2016; Smith, 2002). This statistical tool constructs new axes known as principal  
178 components that are linear combinations of the initial variables. Each principal component is  
179 constructed in a way to maximize the variance, hence capturing as much information as  
180 possible. The contribution of each principal component to the overall data variance can be  
181 visualized by the explained variance ratio. By plotting the principal components with the  
182 highest explained variance ratio, the data can easily be visualized in a two-dimensional graph.  
183 Data belonging to the same category would typically be clustered together in the plot and would  
184 be sufficiently distinct from other clusters. PCA has been used to reduce the dimension of  
185 plastic spectra before passing the principal components as input data into different classifier

186 models (Musu et al., 2019; Yang et al., 2020; Zhu et al., 2019). A sample PCA plot for high  
187 density polyethylene (HDPE) and polyethylene terephthalate (PET) is shown in Fig 1.

188 Soft independent modelling by class analogy (SIMCA) is an extension of PCA used for  
189 classification. For each class, a plane or hyper-plane is constructed from the PCs, and new  
190 samples are classified based upon the distance to the plane or hyper-plane. This method is a  
191 soft classification, as it is possible for each sample to be classified into multiple classes,  
192 depending on the threshold distance for classification (Costa et al., 2017; Wienke et al., 1995).

### 193 **2.2.2 Linear Discrimination Analysis**

194 LDA is related to PCA as a dimensionality reduction tool. However, in LDA, new axes are  
195 constructed in a way that maximizes class separation (Izenman, 2008). This is done by  
196 maximizing the distance between the means of each class while minimizing the scatter of the  
197 dataset within each class. The data is then mapped to the new lower dimension axis. LDA was  
198 used to classify different plastics (Wu et al., 2020) and plastics with different types of  
199 brominated flame retardants (Stefas et al., 2019).

### 200 **2.2.3 Partial Least Square**

201 PLS regression is a statistical method that uses latent variables to study the relationship  
202 between two matrices (Haenlein and Kaplan, 2004) The latent variables are constructed in a  
203 way to find the vector in the X space that corresponds to the vector in the Y space with  
204 maximum variance. When used for classification problem, a variant called PLS discriminant  
205 analysis (PLS-DA) is used, where the Y matrix will be expressed as a dummy matrix of 1 and  
206 0. PLS-DA is one of the more popular chemometric techniques that has been used for  
207 classifying different types of plastics (Calvini et al., 2018; Liu et al., 2019b; Pieszczyk and  
208 Daszykowski, 2019; Saeki et al., 2003; Sato et al., 2002; Silva and Wiebeck, 2019).

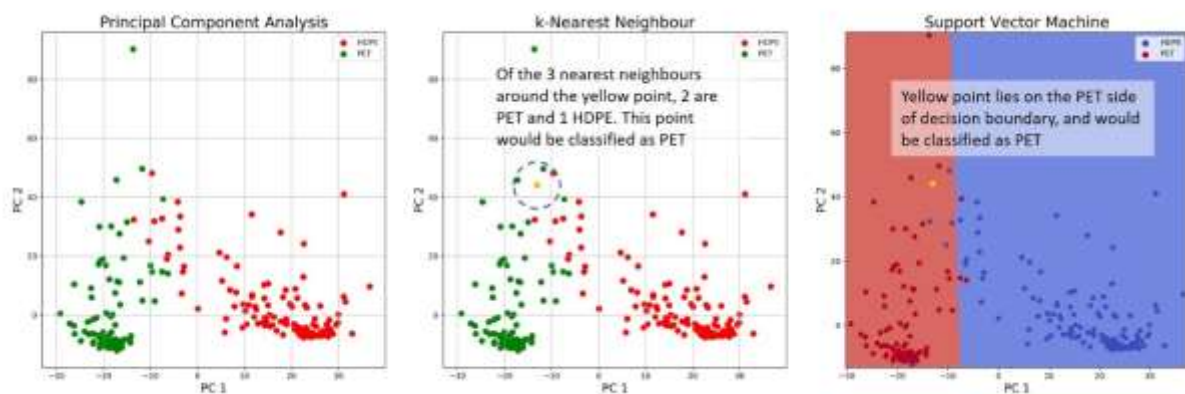
### 209 **2.2.4 k-Nearest Neighbor**

210 k-NN is a classification algorithm which classifies based upon the identity of the k-nearest  
211 neighbors to the new observation (Altman, 1992), where k is a parameter that can be tuned.  
212 The majority class in the k nearest neighbors will determine the class of the new observation.  
213 k-NN can also be combined with PCA for datasets with large dimensions, which is illustrated  
214 in Fig 1. Costa et al., (2017) and Yang et al., (2020) used this algorithm in their works on plastic  
215 classification.



## 216 2.2.5 Support Vector Machine

217 SVM is a classification algorithm that constructs a decision boundary to maximize the distance  
218 between the different classes (Wang, 2005). New samples will then be classified based on the  
219 side of the decision boundary that it falls on in a non-probabilistic manner. Traditionally a  
220 binary classification algorithm, more recent advancement allows for SVM to solve multi-class  
221 classification problems (Lee et al., 2004), including for plastic classification (Musu et al., 2019;  
222 Yang et al., 2020; Yu et al., 2014; Zhu et al., 2019). SVM can also be combined with PCA for  
223 datasets with large dimensions, which is illustrated in Fig 1.



224  
225 **Fig 1.** PCA, k-NN and SVM for chemometric analysis of plastic FTIR data. The dataset from  
226 Chabuka and Kalivas, (2020) was used to build the classifier.

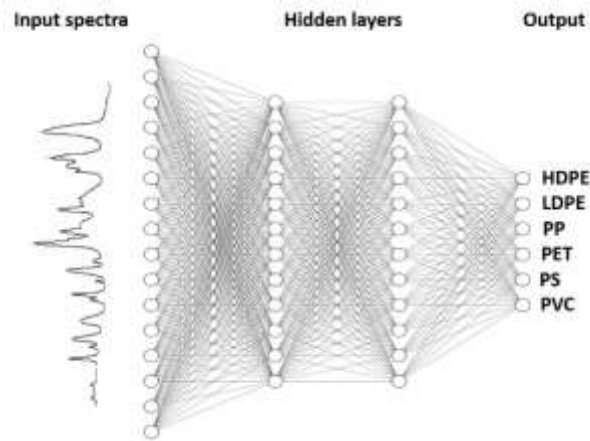
## 227 2.2.6 Random Forests

228 Random forest is an ensemble machine learning technique built using many decision trees  
229 (Breiman, 2001). The output of the random forest algorithm is the mean of the prediction  
230 outputs of all the decision trees. Bagging is employed during the learning process, where each  
231 decision tree is built using different training data. This helps to prevent overfitting to the dataset.  
232 Random forest regression was used with LIBS to quantify the presence of toxic heavy metal  
233 elements in plastics (Liu et al., 2019c).

## 234 2.2.7 Neural Networks

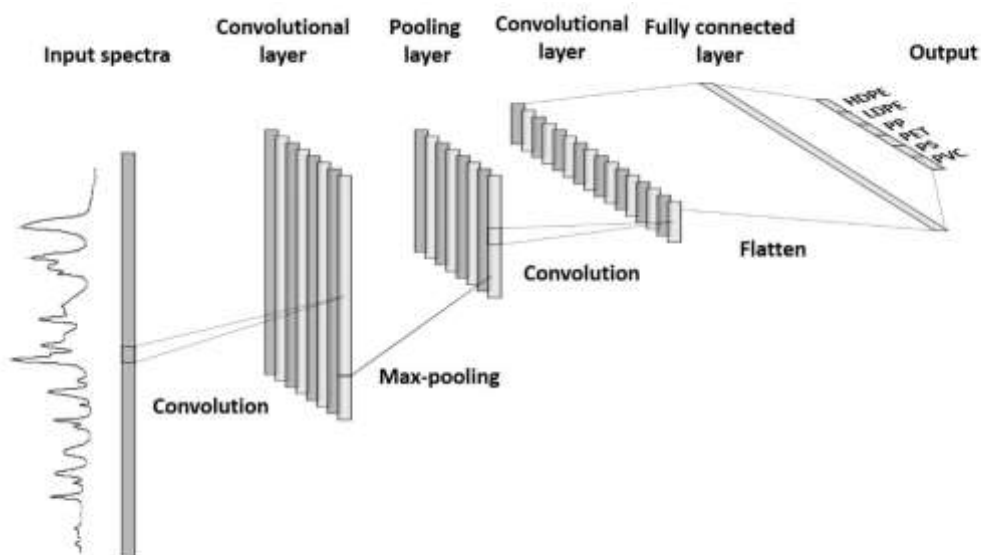
235 Artificial neural networks (ANNs) fall under a branch of machine learning known as deep  
236 learning used for predictive modelling (Krenker et al., 2011). The inputs matrix in the input  
237 layer is mapped to the classified output using neurons in hidden layers. Each of the neurons  
238 contains a function that applies a weight to different part of the input, and together all the  
239 neurons help to learn a complex function. During the training process, the weights are usually

240 adjusted through an iterative backpropagation process to reduce the loss via gradient descent.  
241 Variations of ANN architectures have been widely used in plastic classification (Bae et al.,  
242 2019; Boueri et al., 2011; Junjuri and Gundawar, 2020, 2019; Musu et al., 2019; Roh et al.,  
243 2017; Saeki et al., 2003; Wienke et al., 1995; Yang et al., 2020). A sample ANN architecture  
244 for classifying plastics is shown in Fig 2.



245  
246 **Fig 2.** Sample ANN architecture for plastic classification. The image was built with NN-  
247 SVG.

248 Convolutional neural network (CNN) is one variant of neural network architecture developed  
249 in recent years (Lecun et al., 1998) that has been used with spectra signals (Chen & Wang,  
250 2019; Liu et al., 2017; Ng et al., 2019, 2020; Stiebel et al., 2018; Zhang et al., 2019). CNNs  
251 consist of three types of layers – convolutional layers that extracts features from the input data,  
252 pooling layers that help to reduce the dimension, and fully connected layers that are essentially  
253 ANNs. A sample CNN architecture for classifying plastic is shown in Fig 3.



254

255 **Fig 3.** Sample CNN architecture for plastic classification. The image was built with NN-  
 256 SVG.

257 **2.2.8 K-means Clustering**

258 K-means clustering is an unsupervised machine learning algorithm which groups each  
 259 observation into one of k clusters based on the distance to the centroid of each cluster, where  
 260 k is a hyperparameter to be tuned (Likas et al., 2003). During the learning process, the cluster  
 261 centroids are first randomly defined, and each observation is assigned to the nearest centroid  
 262 based on Euclidean distance. A new centroid is then defined for all the points in each cluster,  
 263 and the process is repeated iteratively until convergence is reached. While K-means clustering  
 264 is not meant to a classification algorithm, polymers of the same type are likely to be clustered  
 265 together, which could result in good polymer sorting if each of the cluster represents a particular  
 266 polymer type. K-mean clustering was used by Guo et al. (2018) to group 20 different polymer  
 267 samples into each own cluster..

268

269 **3. Methodology**

270 The following sections will discuss the results and limitation from previous chemometric  
 271 studies for plastic sorting. This section will outline the characteristics that will be discussed for  
 272 each method.

273 For each study, the methodology and the dataset characteristics will be summarized. In  
 274 particular, for each study we will outline:

- 275 1) Spectroscopic method – IR spectroscopy (including near IR, mid IR and hyperspectral  
 276 imaging), Raman spectroscopy and LIBS.
- 277 2) Samples – the resin type of samples used in the study, which includes the six common  
 278 types of high density polyethylene (HDPE), low density polyethylene (LDPE),  
 279 polypropylene (PP), polyethylene terephthalate (PET), polystyrene (PS), polyvinyl  
 280 chloride (PVC), and other types such as acrylonitrile butadiene styrene (ABS),  
 281 polyamide (PA), polycarbonate (PC), polylactic acid (PLA), polymethyl methacrylate  
 282 (PMMA), polyoxymethylene (POM), polytetrafluoroethylene (PTFE) and  
 283 polyurethane (PU).
- 284 3) Hardware – the instrument and its specifications.
- 285 4) Input – the parts of the chemical data obtained from spectroscopy that is used for  
 286 chemometric analysis.
- 287 5) Software – the software used to run the chemometric tool.
- 288 6) Chemometric tool – tools used to analyze spectroscopic data, including PCA, LDA,  
 289 kNN, PLS, SVM, RF, neural networks.
- 290 7) Results – accuracy, precision and recall (equation 1-3) for classification, root mean  
 291 square error of prediction (RMSEP) for regression.
- 292 8) Dataset characteristics – the data size, color and source of plastic samples (Table S1 to  
 293 S3).

294 The equations used for 7 above are:

$$Accuracy = \frac{TP+TN}{TP+FP+TN+FN} \quad (1)$$

$$Precision = \frac{TP}{TP+FP} \quad (2)$$

$$Recall = \frac{TP}{TP+FN} \quad (3)$$

$$Specificity = \frac{TN}{TN+FP} \quad (4)$$

295 Where *TP* is True Positive, *FP* is False Positive, *TN* is True Negative and *FN* is False Negative.

296 Most chemometric classification studies only report the accuracy of plastic sorting, which is  
 297 useful as a general indication of the model performance. However, whenever possible, this  
 298 review will also derive precision and recall metrics for a more complete picture. Precision  
 299 allows for understanding the level of contamination associated with the sorted polymers.  
 300 However, when some studies report specificity values (equation 4) without a confusion matrix,  
 301 making it impossible to derive the precision value. For those studies, the specificity metrics  
 302 was reported instead. Recall allows for understanding the percentage recovery of polymers of

303 each class. To extract the highest market value from plastic waste, precision should be  
304 prioritized to produce high quality recycled plastic, followed by recall to ensure that potentially  
305 recyclable polymers are not downcycled. However, the recall metric should also be suitably  
306 high such that a fair amount of recyclable plastic can be recovered for the process to be  
307 economically sustainable.

308 The summarized dataset characteristics include the plastic sample color and source. Color on  
309 plastics is due to either organic or inorganic colorants, while the source may give an indication  
310 of possible contamination and degradation. These are important factors that could affect both  
311 identification of the plastic and the recyclability of the plastic. Different colored plastic should  
312 be processed separately during the recycling process for an aesthetically pleasing recycled  
313 product (Ruj et al., 2015). Colorless or white samples have the highest market value as recycled  
314 plastics, since they can be re-dyed with any color (Gabriel and Maulana, 2018). On the other  
315 hand, black samples can only be recycled into black plastics. Contaminants found on plastics  
316 are typically volatile organic compounds (VOCs), which affects the odor quality of the recycled  
317 product (Cabanés et al., 2020; Strangl et al., 2021). Contaminants like detergent could also be  
318 linked to increased thermal degradation effects during the recycling process (Mylläri et al.,  
319 2016). Degradation of plastics are usually associated with formation of carbonyl or hydroxyl  
320 groups on the surface (Canopoli et al., 2020; Pelegrini et al., 2019) which causes changes in  
321 the resulting spectra that could result in misclassification. Degradation also results in decreased  
322 mechanical and rheological properties as compared to virgin plastic (Brouwer et al., 2020).

323

324

325

## 326 **4. Chemometrics with IR**

327 Among the three spectroscopic methods discussed in section 3, IR spectroscopy is the most  
328 widely applied spectroscopic method for chemometric analysis for plastic waste sorting.  
329 Broadly speaking, FTIR spectroscopy can be split into 3 ranges – near-infrared (NIR) with  
330 wavenumber from 14,000 – 4000  $\text{cm}^{-1}$ , mid-infrared (MIR) with wavenumber from 4000 – 400  
331  $\text{cm}^{-1}$  and far infrared (FIR) with wavenumber from 400 – 10  $\text{cm}^{-1}$  (Veerasingam et al., 2020).  
332 Both NIR and MIR are suitable ranges for plastic sorting.

### 333 **4.1 Near Infrared**

334 Table 1 summarizes the methodology and result of works in the literature that utilized NIR for  
335 chemometric analysis of plastic waste.

336 The use of NIR for chemometric analysis of plastic waste is well established, which is evident  
337 from the results (average classification accuracy ranging from 97-100% in the reported works).  
338 Early works identified ANN in combination with NIR as an effective method for sorting  
339 common post-consumer plastic waste with high accuracy (Feldhoff et al., 1997; Huth-Fehre et  
340 al., 1995; Wienke et al., 1995). Highly sensitive detectors in the NIR region by indium gallium  
341 arsenide (InGaAs) based sensors also makes it suitable for use with in-line conveyer belt  
342 systems in the recycling industry (Feldhoff et al., 1995). Much of the research direction  
343 afterwards shifted towards NIR hyperspectral imaging (HSI), which involves generating a 3D  
344 ‘hypercube’ with two spatial dimensions and one spectral dimension (Caporaso et al., 2018).  
345 and will be further covered below in Section 4.1.1. More recent works explored the use of  
346 portable NIR systems and found that they were as effective (Kumar et al., 2014; Rani et al.,  
347 2019; Said et al., 2020; Yang et al., 2020), which opens the door for potential deployment in  
348 decentralized sorting systems such as smart sorting bins.

349 NIR data has also been used to build regression models that provides good age-prediction  
350 accuracy for plastics by subjecting plastic samples to thermal-oxidative aging and extrusion  
351 cycles (Alassali et al., 2020, 2018), which could provide useful information for determining  
352 the recyclability of plastic waste.

353  
354  
355  
356  
357  
358  
359  
360  
361

362 **Table 1:** Summary of NIR chemometrics study for plastic waste sorting.

Reference	Samples	Hardware	Input	Software	Chemometric Tool	Accuracy	Precision	Recall	Main Misclassification
1 (Huth-Fehre et al., 1995; Wienke et al., 1995)	PE, PP, PET, PS, PVC	PolyTec X-DAP, InGaAs detector	Full NIR spectrum (825 – 1700nm)	ARTHUR MATLAB	SIMCA ANN	Median sorting purity of 98%			-
2 (Feldhoff et al., 1997)	PE, PP, PET, PS, PVC	PolyTec X-DAP, InGaAs detector	Full NIR spectrum (825 – 1700nm)	Not stated	ANN	Overall 97%			PE and PP
3 (Saeki et al., 2003)	HDPE, LDPE, LLDPE	PlaScan-SH (Opt Research Inc., Japan)	Second-derivative of full NIR spectrum (1100-2200nm)	Pirouette, NEUROSI M/L	PCR PLS ANN		RMSEP of 0.0043 RMSEP of 0.0031 RMSEP of 0.00026		-
						PE density range 0.898-0.962 g cm <sup>-3</sup>			
4 (Zhao and Chen, 2015)	PE, PP, ABS, PMMA	Jiaoda spectrometer	First 3 Principal components for NIR spectrum (900-1700nm)	Not stated	Mahalanobis distance	88.9-100% (Overall 97%)	88.9-100% (Overall 97%)	90.9-100% (Overall 97%)	ABS predicted as PP

5 (Zhu et al., 2019)	PE, PP, PET, PS, ABS, PMMA	NIR optical fiber spectrometer with InGaAs detector	First 7 principal components for NIR spectrum (1000-1700nm)	LabVIEW	PCA-SVM	85-100% (Overall 97.5%)	87-100% (Overall 97.8%)	85 – 100% (Overall 97.5%)	PE predicted as PP
6 (Rani et al., 2019)	PE, PP, PET, PS, PVC	MicroNIR On-site	Full NIR spectrum (900-1700nm)	MicroNIR TM Pro v3.0 software	PLS-DA	Overall Accuracy: 100%			
7 (Wu et al., 2020)	PP, PS, ABS, ABS/PC blend	Ocean Optics NIR512	Part of NIR spectrum (1084-1562nm)	Python	PLS-DA PCA-LDA	99.5-100% (Overall 99.9%)	99.1-100% (Overall 99.9%)	99.5-100% (Overall 99.9%)	-
8 (Yang et al., 2020)	PE, PP, PET, PVC, PS, ABS, PC White and transparent samples	Pynect NIR-S-G1 NIR handheld spectrometer	Full NIR spectrum (900-1700nm)	Python (PyCharm)	PCA-SVM	100% (All)	100% (All)	100% (All)	
					PCA-KNN	100% (Transparent) 99.95% (White)	100% (Transparent) 99.96% (White)	100% (Transparent) 99.95% (White)	-
					PCA-ANN	100% (Transparent) 99.94% (White)	100% (Transparent) 99.94% (White)	100% (Transparent) 99.94% (White)	
9 (Said et al., 2020)	PP, PET	Miniaturized MEMS FTIR spectrometer	First 2 latent variables for NIR spectrum (1350-2500nm)	Not stated	PLS, KNN	Overall Accuracy: 100%			-



#### 364 **4.1.1 Near Infrared Hyperspectral Imaging**

365 Hyperspectral imaging (HSI) in the NIR range have started to be adopted by some industries  
366 (WRAP, 2016), The imaging capabilities help to provide information about the purity of plastic  
367 samples through the spatial distribution of different spectra on the sample. Some of the NIR  
368 hyperspectral imaging technologies currently in the market includes the Specim FX17 (Specim,  
369 2020a), KUSTAx.x MSI series (LLA Instruments, n.d.), Pika NIR series (Resonon, 2020) and  
370 INNO-SPEC RedEye (Acal Bfi, 2015a), some of which have been utilized in the reported  
371 literature (Calvini et al., 2018; Pieszczyk and Daszykowski, 2019). Table 2 summarizes the  
372 methodology and result of the work in the literature that utilized HSI-NIR for chemometric  
373 analysis of plastic waste.

374 Initial work in this field using PCA found clear separation between two different groups of  
375 polymers such as PE and PP, PE and PET or PET and PLA (De Biasio et al., 2010; Serranti et  
376 al., 2012, 2011; Ulrici et al., 2013). More recently, 100% accuracy was obtained in classifying  
377 PE and PP using PLS-DA (Serranti et al., 2015). With an increase in scope of polymer class  
378 considered, there is a slight drop in overall results (Calvini et al., 2018; Karaca et al., 2013;  
379 Pieszczyk and Daszykowski, 2019; Stiebel et al., 2018) as compared to the results shown in  
380 Table 1 with the use of NIR spectrometer, which could be partly due to poorer resolutions in  
381 HSI-NIR spectra. However, the accuracies reflect pixel accuracies, rather than sample  
382 accuracies. In most cases, the majority of pixels in the plastic sample is correctly classified,  
383 which would have likely resulted in positive identification of the sample. Furthermore, it was  
384 also found that using selected bands representing 10% of the initial input data do not  
385 compromise the overall performance (Kim and Kim, 2016). To further improve the sorting  
386 accuracy, the effect of different pre-processing methods can be explored, as it can significantly  
387 influence the final results (Galdón-Navarro et al., 2018).

388

389 More recent works have attempted to make use of the spatial information captured within HSI-  
390 NIR for more detailed chemometric analysis, such as in detecting contamination in plastics such  
391 as bromine flame retardants (Bonifazi et al., 2020; Caballero et al., 2019), identifying multi-  
392 layered polymers (Bonifazi et al., 2021; Chen et al., 2021b; Stiebel et al., 2018) and  
393 distinguishing between plastic of varying degradation levels (Chen et al., 2021a),

394

395 While the research in this field is mature, there remains some gaps in this field. Most of the  
396 work has focused on variations of the six common plastic – HDPE, LDPE, PET, PP, PS and

397 PVC. In reality, the mix of plastic waste would be much more heterogenous, which may affect  
398 the accuracy of chemometric models. The use of NIR in chemometric analysis of polyolefins  
399 should also be better understood, as not many works have split the class of PE in HDPE and  
400 LDPE (Calvini et al., 2018; Karaca et al., 2013; Saeki et al., 2003; Stiebel et al., 2018). Some  
401 work also reported mislabeling of some PE and PP samples (Pieszczyk and Daszykowski, 2019;  
402 Zhu et al., 2019). There is also lack of an open-sourced NIR polymer database, which limits  
403 further research in this field.

404

405 Furthermore, there are glaring limitations of NIR in sorting plastic waste. One of the major  
406 drawbacks with NIR is the inability to differentiate black plastics, as electromagnetic radiation  
407 in the NIR region is strongly absorbed by black material due to its proximity to the visible light  
408 range (Becker et al., 2017). Furthermore, NIR is composed of overtones and combination bands  
409 of different functional groups such as C-H, N-H and O-H, resulting in weaker spectral features  
410 that may present difficulties towards unique identification (Vázquez-Guardado et al., 2015). In  
411 order to manage the heterogenous plastic waste at recycling facilities, NIR data can be  
412 supplemented with data from other non-destructive spectroscopic sets like MIR, Raman and  
413 LIBS, which will be covered in later sections.

414

415 **Table 2:** Summary of HSI-NIR chemometrics study for plastic waste sorting.

Reference	Samples	Hardware	Input	Software	Chemometric Tool	Accuracy	Precision	Recall	Main misclassification
1 (De Biasio et al., 2010)	PE, PP	NIR scanner from Titech	HSI-NIR (1000-2500nm)	Not stated	PCA	PE and PP can be distinguished, different PP products can be distinguished as well.			-
2 (Serranti et al., 2011)	PE, PET	Specim NIR Spectral Camera with InGaAs detector	HSI-NIR (1000-1700nm)	Spectral Scanner v2.3	PCA	PE and PP can be distinguished from other contaminants (aluminum, wood, foam)			-
3 (Serranti et al., 2012)	PE, PP	Specim NIR Spectral Camera with InGaAs detector	HSI-NIR (1000-1700nm)	Spectral Scanner v2.3	PLS-DA	Not stated	94-95%	94-95%	
4 (Karaca et al., 2013)	HDPE, LDPE, PP, PET, PVC, PS	SWIR Camera	HSI-NIR (1000-2500nm)	Self-developed	SVM	93.5-96.9%	Not stated	Not stated	LDPE predicted as HDPE
5 (Ulrici et al., 2013)	PET, PLA	Specim ImSpector N17	HSI-NIR (1000-1700nm)	Not stated	PLS-DA	98.7-100%	Not stated	Not stated	-

---

6 (Bonifazi et al., 2014)	PE, PP, PET, PS, PVC	Specim ImSpector N17	HSI-NIR (1000-1700nm)	MATLAB	PLS-DA	Not stated	99.8-100%	100%	-
7 (Serranti et al., 2015)	PE, PP	Specim ImSpector N17	HSI-NIR (1000-1700nm)	MATLAB	PLS-DA	100%	100%	100%	-
8 (Calvini et al., 2018)	HDPE, LDPE, PP, PET, PVC, PS, ABS, PLA	HSI Camera KUSTA1.9M SI, LLA Instruments with InGaAs detector Zeiss f/2.4, 10 mm optical lens	HSI-NIR (1330 – 1900nm)	MATLAB	Soft PLS-DA	98.4%	Specificity: 97.4-100%	92.1-100%	
9 (Stiebel et al., 2018)	HDPE, LDPE, PP, PET, PVC, PS, ABS and mixed samples	hyperspectral NIR-camera	HSI-NIR (900-1700nm)	Python (Tensorflow/Keras)	CNN (Hypnet)	92%	Not stated	Not stated	
10 (Pieszczek and Daszykowski, 2019)	HDPE, PP, PS, PET, ABS	Specim FX17e camera with InGaAs detector	HSI-NIR (1000-1700nm)	MATLAB	OC-PLS	Not stated	Specificity: 99.5-99.9%	93.4-98.6%	PP predicted as HDPE

---

11 (Serranti et al., 2020)	HDPE, PP White, red, orange, yellow green, blue samples	Specim ImSpector N25E imaging spectrograph, ImSpector V10E VISOBUR canera	HSI-NIR (1000-2500nm)	MATLAB	PLS-DA	Not stated	<u>Type class</u> 100%	<u>Type class</u> 100%	-
12 (Chen et al., 2021a)	PE, PP, PET, PS Varying degradation	Helios-G2-320 NIR sensor from EVK DI Kerschhaggl GmbH	HSI-NIR (930-1700nm)	Python Scikit-learn	PLS-DA	Postconsumer plastic: 99 – 99.8% Landfill plastic: 89.8 – 99.5% Marine plastic: 75.5 – 90.1%	<u>Color class</u> 92.6-100%	<u>Color class</u> 98.9-100%	-
							<u>Not stated</u>	<u>Not stated</u>	-

## 417 **4.2 Mid Infrared**

418 The MIR region contains fundamental vibrational bands with distinct spectral features and is  
419 also known as the molecular fingerprint region. Since the MIR region is sufficiently distinct  
420 from the visible light region, it is not affected by black plastics (Becker et al., 2017; Signoret  
421 et al., 2020). In addition, MIR spectroscopy is less affected by surface morphology and color  
422 of the plastic sample as compared to NIR spectroscopy (Vázquez-Guardado et al., 2015).  
423 Despite the above listed advantages that MIR has over NIR, the use of this technology in plastic  
424 recycling applications has been limited by the spectral acquisition speed with less sensitive  
425 photodetectors, two of the most commonly used being deuterated triglycine sulfate and  
426 mercury cadmium telluride (Kempfert et al., 2001). Becker et al., (2017) managed to employ a  
427 photon-up conversion technique to convert MIR photons to higher energy NIR signal, which  
428 can be picked up using a more sensitive InGaAs sensor, which improves the economic viability.

429 Table 3 summarizes the methodology and result of two works in the literature that utilized MIR  
430 for chemometric analysis of plastic waste. Both studies suggest 100% sorting accuracy, but a  
431 further study in this field would be needed to better understand the effectiveness of MIR  
432 technology for plastic sorting. This includes broadening the types of chemometric tools and  
433 plastic samples used. Some works have begun building up MIR spectral characteristics for  
434 polyolefins and styrenic polymers towards potential industrial application (Signoret et al.,  
435 2019a, 2019b). There are also open-sourced MIR polymer data that can be used for further  
436 chemometric studies (Baskaran and Sathivelu, 2020; Chabuka and Kalivas, 2020; Cowger et  
437 al., 2021).

438

### 439 **4.2.1 Mid Infrared Hyperspectral Imaging**

440 Recent technological improvements have led to MIR-HSI being introduced into the market,  
441 allowing for potential application in an industrial setting (Signoret et al., 2019a, 2019b). Some  
442 of the products on the market now includes the Specim FX50 (Specim, 2020b) and INNO-  
443 SPEC BlackEye (Acal Bfi, 2015b). MIR-HSI was recently explored via cautious machine  
444 learning method, such that samples with high uncertainty in the prediction are rejected. The  
445 study method was employed to sort styrenic polymers and polyolefins with higher purity  
446 (Jacquin et al., 2021).

447

448

449 **Table 3:** Summary of MIR chemometrics study for plastic waste sorting.

Reference	Samples	Hardware	Input	Software	Chemometric Tool	Accuracy	Precision	Recall
1 (Kassouf et al., 2014)	HDPE, LDPE, PP, PET, PS, PLA	Bruker ATR FTIR	Full MIR spectrum (600-4000cm <sup>-1</sup> )	MATLAB	ICA	Plastics can be discriminated from each other		
2 (Bae et al., 2019)	PP, PET, PS	Bruker ATR FTIR	Extracted peaks from MIR spectrum (600-2000cm <sup>-1</sup> )	WEKA 3.8	RBFNN	99-100%	Not stated	Not stated

450

## 451 **5. Chemometrics with Raman**

452 Raman spectroscopy is the second of the three spectroscopic methods introduced in section 3  
453 that could potentially be combined with chemometric tool towards plastic waste sorting. Raman  
454 has emerged as a technique that overcomes the shortcomings of NIR, such as inability to handle  
455 black plastics and poor spectral resolution in a rapid fashion (Chen et al., 2017; Musu et al.,  
456 2019; Tsuchida et al., 2009). Furthermore, Raman spectroscopy is often described as a  
457 complementary technique to MIR, as vibrational modes that are IR active are often not Raman  
458 active, and vice versa. However, the use of Raman spectroscopy for plastic identification is  
459 much less widespread when compared to IR, due to background fluorescence which can often  
460 overshadow certain peaks of interest (Araujo et al., 2018; Dong et al., 2020). Table 4  
461 summarizes the methodology and result of works in the literature that utilized Raman  
462 spectroscopy for chemometric analysis of plastic waste.

463 Florestan et al. (1994) first identified the potential for Raman spectroscopy to be used to  
464 distinctly identify HDPE, PP, PET and PVC through comparison to a reference library. The  
465 authors also found that PP with fillers could be differentiated from pure PP from the Raman  
466 spectra. Allen et al. (1999) later expanded the polymer scope to include LDPE and PS, but  
467 could not achieve good overall accuracy. With the rise in popularity of machine learning  
468 models, more recent works have demonstrated the potential of chemometric tools like neural  
469 networks and SVM for analysis of Raman data for qualitative analysis of plastic, achieving  
470 between 94-100% accuracy in classifying plastic (Chen et al., 2017; Musu et al., 2019; Roh et  
471 al., 2017; Tsuchida et al., 2009).

472 Chemometric analysis of Raman spectra has also been shown to be effective in sorting  
473 polyethylene of different densities, as the intensities of CH<sub>2</sub> scissoring and wagging mode in  
474 the Raman spectrum are sensitive to the crystallinity of PE (Sato et al., 2002). Allen et al. (1999)  
475 first demonstrated this with 100% correct identification of both HDPE and LDPE in his work,  
476 even while the identification of other polymers was not as effective. Other work demonstrates  
477 the quantitative analysis of the density through PLS regression models, allowing for finer  
478 distinction between HDPE, LDPE and LLDPE (Sato et al., 2002) or different HDPE/LDPE  
479 blends (Silva and Wiebeck, 2019).

480 Despite the demonstrated potential, there are still some gaps that need to be addressed. Most  
481 of these works extracted specific peaks for the polymer of interest to build the classification  
482 model (Musu et al., 2019; Roh et al., 2017; Tsuchida et al., 2009). This may limit the potential



483 use in a potential industry application, where a much wider variety of polymer is encountered.  
484 Polymers that were not included in the training data could be falsely labeled, resulting in  
485 contamination that affects the quality of recycled plastic. Furthermore, no further information  
486 about the quality of the plastics, such as presence of additives and contamination, can be  
487 obtained from only studying the extracted peaks. While colored pigments can result in  
488 additional peaks or broad fluorescence bands (Florestan et al., 1994; Marica et al., 2019), the  
489 effect of different colored plastics on the performance of chemometric analysis with Raman  
490 spectra is also not well studied, as most of the works focused on plastic samples with largely  
491 homogenous colors (Chen et al., 2017; Roh et al., 2017) (Table S2).

492 Further work in this field should focus on broadening the scope of Raman spectra to a wider  
493 variety of polymer samples and colors that more closely resembles heterogenous plastic waste  
494 received at a recycling plant. There are currently several open-sourced Raman databases that  
495 could be utilized for such chemometric studies (Cowger et al., 2021; Dong et al., 2020; Munno  
496 et al., 2020). The potential for Raman spectra to be used with chemometric analysis for  
497 determining contamination and degradation levels within polymer samples have also not been  
498 studied.

499 **Table 4:** Summary of Raman chemometrics study for plastic waste sorting.

Reference	Samples	Hardware	Input	Software	Chemometric Tool	Accuracy	Precision	Recall
1 (Florestan et al., 1994)	HDPE, PP, PET, PVC	Bruker IFS 66 spectrometer with 300 mW YAG laser	Full Spectrum (400-4000cm <sup>-1</sup> )	In-built software	Library searching		Not stated	
2 (Allen et al., 1999)	HDPE, LDPE, PP, PET, PVC, PS	Spex Raman Spectrometer with CCD, 514.5 nm laser	Full Spectrum (850-1800cm <sup>-1</sup> )	SpectraMax (in-built software)	PCA-kNN Library searching	100% 38 – 100% (Overall 87%)	Not stated	Not stated
3 (Sato et al., 2002)	HDPE, LDPE, LLDPE	JASCO NRS 2001 Raman spectrometer with CCD, 514.5 nm laser	Full Spectrum (600-1800cm <sup>-1</sup> )	Unscrambler	PLS	RMSEP of 0.0015 for PE density (range from 0.918 to 0.964 g/cm <sup>3</sup> )		
4 (Tsuchida et al., 2009)	PP, PS, ABS	Homemade Raman Apparatus with CCD, 785 nm laser diode	Extracted peaks from full spectrum (300-3500cm <sup>-1</sup> )	R	Multivariate Analysis	Overall Accuracy: 94%	Not stated	Not stated
5 (Chen et al., 2017)	PE, PP, PET, PVC, PS, PMMA, POM	LabRAM HR Evolution microscopic confocal	First seven principal components of full spectrum	Not stated	SVM	Overall Accuracy: 100%		

6 (Roh et al., 2017)	PP, PET, PS	Raman spectrometer, 532 nm laser Not stated	(200-2400cm <sup>-1</sup> ) Extracted peaks from full spectrum (200-3000cm <sup>-1</sup> )	Not stated	FRBFNN	Overall Accuracy: 95%	Not stated	Not stated
7 (Musu et al., 2019)	PP, PS, ABS	Homemade Raman Apparatus with CCD, 785 nm laser diode	Extracted peaks from full spectrum (100-3300cm <sup>-1</sup> )	R (e1071 library) Python (TensorFlow /Keras)	PCA-SVM ANN	Overall Accuracy: 100%		
8 (Silva and Wiebeck, 2019)	HDPE/LDPE blends	Confocal Raman Microscope Alpha300 R, 532nm laser	Extracted peaks from full spectrum (210-3875cm <sup>-1</sup> )	MATLAB	PLS	RMSEP of 4.062 wt% of LDPE (range from 0 to 100%)		

## 501 **6. Chemometrics with LIBS**

502 LIBS is the last of the three spectroscopic methods introduced in section 3. When compared to  
503 IR and Raman, LIBS is a relatively newer spectroscopic method that has, in recent years, been  
504 used for chemometric analysis of plastic waste in a laboratory setting. (Liu et al., 2019a; Zeng  
505 et al., 2021). Since LIBS reflects the elemental composition of the sample, it does not suffer  
506 from the drawback of insensitivity to specific chemical bonds with IR or Raman spectroscopy.  
507 The relative intensity of spectral lines within a LIBS spectrum is indicative of the elemental  
508 ratio within the polymers, which can be used to differentiate different types of polymers. The  
509 ability to detect different types of elements broaden the range of plastics that can be identified,  
510 including polymers such as PTFE, PU, PA, PMMA and POM that were hardly or never  
511 explored using Raman and IR spectroscopy. Table 5 summarizes the methodology and result  
512 of works in the literature that utilized LIBS for chemometric analysis of plastic waste.

513 LIBS was realized as a technique that could be used for sorting common post-consumer plastics  
514 (HDPE, LDPE, PET, PP, PS, PVC) as each polymer had different C/H ratios using a simple  
515 calibration curve (Anzano et al., 2008; Gondal and Siddiqui, 2007). Some mixed success was  
516 subsequently achieved in sorting via LIBS data through Euclidean distance comparison to a  
517 reference library (Anzano et al., 2010). Banaee and Tavassoli (2012) later achieved good  
518 overall accuracy of 99% with the common post-consumer plastics using statistical methods.  
519 Since then, more recent works focused on expanding the scope of plastic for classification with  
520 various more modern machine learning methods. LIBS has also been shown to distinguish  
521 between different polymer samples of the same resin type (Guo et al., 2018; Tang et al., 2018;  
522 Yan et al., 2021), highlighting the potential in precise sorting of plastic waste. Most recently,  
523 a CNN-based approach was explored, which was found to out perform other machine learning  
524 models like ANN, SVM and kNN (Peng et al., 2021).

525 The studies using chemometrics with LIBS show good overall results, with 13 out of the 16  
526 reviewed works reporting average accuracies of over 95%. The works that report high  
527 accuracies across a wide range of polymer types employed either features selection methods  
528 such as variable importance (Liu et al., 2019b) or adjusted spectral weightings (Tang et al.,  
529 2018; Yu et al., 2014). These techniques allow for accentuating weak spectral features such as  
530 CN, C<sub>2</sub> and O emission lines (Yu et al., 2014).

531 As an elemental analysis technique, chemometric analysis of LIBS can also be used to detect  
532 the presence of inorganic elements that could be linked to different additives, such as metallic-

533 based colorants or fillers (Ángel Aguirre et al., 2013; Boueri et al., 2011; Godoi et al., 2011;  
534 Liu et al., 2019c). The chemometric methods used include ANN, RF, PLS-DA, SIMCA and  
535 KNN. Atomic spectral emissions associated with halogens like Cl and Br lie in a less sensitive  
536 region in the spectra, making it hard to observe without more specialized equipment. However,  
537 LIBS has also been used to some success to detect presence of brominated flame retardants  
538 (Stefas et al., 2019) and chlorine containing polymers (Huber et al., 2014; Vahid Dastjerdi et  
539 al., 2018).

540 Despite the promising results, there are some limitations associated with LIBS as an elemental  
541 analysis technique since information on the molecular structure is lost. Hence, polymers with  
542 similar elemental compositions could be hard to distinguish, such as PS and ABS (Costa et al.,  
543 2017) or PS and PC (Tang et al., 2018). While is an absence of oxygen in PS, the difficulty in  
544 sorting PC and PS was attributed to the similar relative content of C and H in both polymers,  
545 and the fact that experiments were ran in open air, where oxygen from the atmosphere  
546 interfered with the spectrum results. Supplementing LIBS data with IR or Raman spectroscopic  
547 data could potentially help to address this limitation. There could be some challenge with  
548 distinguishing between HDPE and LDPE as well, since both polymers are chemically similar.  
549 Some works have found success in this area (Costa and Pereira, 2020; Junjuri and Gundawar,  
550 2020, 2019; Liu et al., 2019b) which could be due to the difference in additives used in both  
551 types of polymers (Arias et al., 2009).

552 In addition, some gaps remain in the literature. Firstly, a large majority of the works used very  
553 limited samples, often just using spectra taken from different locations of the same sample for  
554 each polymer type (Table S3). However, polymers of the same resin type from different  
555 suppliers can differ in the LIBS spectra due to presence of different additives (Peng et al., 2021).  
556 A more comprehensive study with a larger sample size would provide higher confidence that  
557 the results would generalize well to an industry. Secondly, despite the shift towards the use of  
558 LIBS for analyzing post-consumer plastics in recent years, there is a lack of open-sourced LIBS  
559 database, which limits further work in the field. Lastly, while LIBS has been used to detect the  
560 presence of metal contaminants, the potential application in predicting degradation levels are  
561 not well understood. Since degradation is associated with formation of oxygenated groups like  
562 carbonyl and hydroxyl, the O/C emission lines ratio could be a good indication of degradation  
563 levels.

564 **Table 5.** Summary of LIBS chemometrics study for plastic waste sorting.

Reference	Samples	Hardware	Spectral Lines	Software	Chemometric Tool	Accuracy	Precision	Recall	Main misclassification
1 (Anzano et al., 2010)	PE, PP, PET, PS	Q switched Nd: YAG Laser at 532nm, ICCD	Full Spectrum	Microsoft Excel	Euclidean Distance	67 – 100% (Overall 87%)	Not stated	Not stated	
2 (Grégoire et al., 2011)	PE, PP, PS, PA, PC	fourth-harmonic Nd:YAG laser, ICCD	C, H, N, O, CN, C <sub>2</sub>	AnaLIBS (IVEA)	PCA	Polymers can be distinguished from each other			
3 (Boueri et al., 2011)	PE, PP, PVC, PTFE, POM, PA, PC, PMMA	Quadrupled Nd :YAG pulsed laser 266nm, ICCD	C, H, N, O, F, Cl Na, Mg, K, Ca, Ti CN	In-built software	ANN	81 – 100% (Overall 96%)	Not stated	Not stated	
4 (Banaee and Tavassoli, 2012)	HDPE, LPDE, PP, PET, PS, PVC	Q switched Nd: YAG Laser at 1064nm, ICCD	C, H, N, O, Cl, CN, C <sub>2</sub>	SPSS 17.0	Discriminant Function Analysis	94 – 100% (Average 99%)	96.2-100% (Average 98.8%)	94 – 100% (Average 99%)	PP predicted as HDPE and LDPE
5 (Yu et al., 2014)	PE, PP, PVC, PS, ABS, PTFE, PA, PC, PMMA, PU, POM	Q switched Nd: YAG Laser at 532nm, ICCD	C, H, N, O, F, Cl Na, Mg, K, Ca, Ti CN, C <sub>2</sub>	MATLAB	SVM, with adjusted spectral weightings	Overall accuracy: 100%			

6 (Costa et al., 2017)	PE, PP, ABS/PS, PA, PC	Nd:YAG Laser, CCD spectrometer	C, H, N, O	Aurora Software	KNN	91 – 100% (Overall 98%)	97 – 98% (Overall 97%)	91 – 100% (Overall 98%)
					SIMCA	89 – 96% (Overall 92%)	91 – 93% (Overall 92%)	89 – 96% (Overall 92%)
7 (Roh et al., 2018)	PP, PS, ABS	Not stated	Extracted features using PCA and ICA	Not stated	RBFNN	95.83%	Not stated	Not stated
8 (Vahid Dastjerdi et al., 2018)	PVC and others (PE, PP, PS, PMMA)	Q switched Nd: YAG Laser at 1064nm	C, N, C <sub>2</sub>	MATLAB	SVM	90.5% (Separating PVC from other polymers)	Not stated	Not stated
9 (Guo et al., 2018)	PE, PP, PVC, PS, ABS, PTFE, PA, PC, PMMA, PU, POM	Q switched Nd: YAG Laser at 532nm, ICCD	C, H, O CN	MATLAB	K-means clustering	99.6%	Not stated	Not stated
10 (Tang et al., 2018)	PE, PP, PVC, PS, ABS, PTFE, PA, PC, PMMA, PU, POM	Q switched Nd: YAG Laser at 532nm, ICCD	C, H, N, O CN, C <sub>2</sub>	MATLAB	SOM with adjusted spectral weightings, K-means	96 – 100% (Overall: 99%)	Not stated	Not stated

11 (Stefas et al., 2019)	ABS (with different additives)	Q switched Nd: YAG Laser	Full spectrum	Python Scikit-learn	LDA		Overall accuracy: 100%		
12 (Junjuri et al., 2019)	HDPE, LDPE, PP, PET, PS, ABS, PC, HIPS,	Q switched Nd: YAG Laser at 532nm, ICCD	Full spectrum	In-built Labview programme	PLS-DA	87.2 – 97.2% (Overall 93.3%)	Not stated	Not stated	
13 (Liu et al., 2019b)	HDPE, LDPE, PP, PVC, PS, ABS, PTFE, PC, PMMA, PU, POM	Solid-state Q-switched laser at 1064 nm	18 latent variables selected from full spectrum	MATLAB	PLS-DA	99.55%	Not stated	Not stated	
14 (Junjuri and Gundawar, 2019)	HDPE, LDPE, PP, PET, PS	Ti:Sapphire laser System at 800nm, ICCD	C, H, N, O, Na, Mg, K, Ti, CN, C <sub>2</sub> , NH	MATLAB	ANN	97.8-100% (Overall 99.3%)	97.8-100% (Overall 99.3%)	97.8-100% (Overall 99.3%)	LDPE predicted as HDPE
15 (Junjuri and Gundawar, 2020)	HDPE, LDPE, PP, PET, PS, ABS, PC, HIPS,	Q switched Nd: YAG Laser at 532nm, ICCD	C, H, N, O, Na, Mg, K, Ca, Ti, CN, C <sub>2</sub> , NH	In-built Labview programme	ANN with feature selection	95.1 – 99% (Overall 97%)	Not stated	Not stated	
16 (Yan et al., 2021)	PE, PP, PVC, PS, ABS, PTFE,	Q switched Nd: YAG Laser at	20 PCs from full spectrum	MATLAB	PCA-kNN	92.1 – 100% (Overall 99.6%)	Not stated	Not stated	



---

	PA, PC, PMMA, PU, POM	532nm, ICCD						
17 (Peng et al., 2021)	PVC, ABS, PA, PMMA	Q switched Nd: YAG Laser at 532nm, ICCD	Full spectrum	Not stated	CNN (ResNet)	100%	100%	100%

---

565

## 566 **7. Discussion**

567 The review of relevant literature revealed the following gaps in the field: 1) scope of plastic  
568 covered, 2) hybrid spectroscopic methods, 3) open-sourced database and 4) deep learning  
569 methods. They will be covered in detail from sections 7.1-7.4.

### 570 **7.1 Scope of Plastic Covered**

571 The type of plastic considered in current studies is limited largely to some of the most common  
572 materials found in post-consumer plastic waste. Furthermore, some studies typically focus on  
573 just separating between very specific choices of plastic type. In reality, post-consumer plastic  
574 waste can also contain some less common polymers such as natural polymers and specialized  
575 engineering polymers. Exclusion of these polymers from the dataset may result in  
576 misclassification into potentially recyclable polymer classes, lowering the quality of the  
577 recycled plastic. Hence, less common plastics should also be included in future studies in order  
578 to build a more robust chemometric model for dealing with heterogenous polymer mix.

579 Further sorting of plastic types based on quality characteristics like contamination and  
580 degradation level, which are important considerations for the recyclability, have also not been  
581 well studied. These characteristics would be especially important for widely recyclable plastics  
582 like HDPE, PET and PP. Some preliminary works suggests that LIBS could be used to detect  
583 the presence of additives and contaminants in plastic waste, such as chlorine containing  
584 polymers (Huber et al., 2014), heavy metals (Costa and Pereira, 2020; Godoi et al., 2011) and  
585 brominated flame retardants (Stefas et al., 2019). Degradation typically results in formation of  
586 carbonyl or hydroxyl groups, leading to increased O/C ratio which can be picked up using NIR  
587 or MIR (Alassali et al., 2020, 2018; Dong et al., 2020).

### 588 **7.2 Hybrid Spectroscopic Methods**

589 While NIR is the predominant spectroscopic method used in the recycling industry today, other  
590 discussed spectroscopic methods (MIR, Raman, LIBS) have shown good potential as well, with  
591 most of the reviewed works reporting similar accuracies (well above 95%) to NIR studies.  
592 Since most of the spectra for different plastics are distinctly different, these results come as no  
593 surprise. Each of the methods have their own benefits and drawbacks, which are summarised  
594 in Table 6. NIR is the cheapest spectroscopic method of the four, but suffers in spectra  
595 resolution and dealing with black plastics (Beigbeder et al., 2013). On the flipside, MIR is not  
596 limited by black plastics, but has a much slower speed of spectrum acquisition (Kassouf et al.,

2014). For IR spectroscopy, the presence of water can affect the IR spectrum due to strong absorption of IR radiation by O-H bonds. This effect is more pronounced in MIR than in NIR (Pasquini, 2018), where the O-H peaks could completely overlay other peaks of interest, most notably characteristic C-H peaks for different polymers (Primpke et al., 2020). In addition, sorting between HDPE and LDPE using IR spectroscopy could be potentially problematic, requiring some pre-processing such as using second derivatives before the difference in spectral features can be discerned (Saeki et al., 2003). The difference in spectral features between HDPE and LDPE are more distinct with Raman spectroscopy (Allen et al., 1999), but the method suffers from low sensitivity and interference of fluorescence (Dong et al., 2020). LIBS has the potential to identify the largest scope of plastics as compared to other three method, while also providing information on metallic contaminants (Ángel Aguirre et al., 2013; Liu et al., 2019c). However, LIBS spectra do not contain information about the molecular structure, and may struggle in distinguishing polymers with similar chemical formula (Costa et al., 2017).

**Table 6.** Comparison of different spectroscopic methods

<b>Spectroscopic Method</b>	<b>Advantages</b>	<b>Disadvantages</b>	<b>Cost (Portable options)</b>
NIR	<ul style="list-style-type: none"> <li>• Rapid and cost-effective</li> <li>• Well-researched</li> </ul>	<ul style="list-style-type: none"> <li>• Weak spectral features</li> <li>• Unable to identify black plastics</li> <li>• Spectra affected by presence of water</li> </ul>	<u>NIR Spectrometer</u> Ocean Insight NIRQuest - \$17,000 (Ocean Insights, n.d.)
			StellarCASE-NIR - \$20,000 (StellarNet Inc, n.d.)
			<u>NIR HSI</u> Specim FX17 – \$42,500 (Stuart et al., 2020)
MIR	<ul style="list-style-type: none"> <li>• Intense spectral features</li> <li>• Not limited by black plastics</li> </ul>	<ul style="list-style-type: none"> <li>• Slow spectral acquisition</li> <li>• Spectra strongly affected by presence of water</li> </ul>	<u>MIR HSI</u> Specim FX50 - \$200,000 (Stuart et al., 2020)
Raman	<ul style="list-style-type: none"> <li>• Able to distinguish PE of different densities</li> </ul>	<ul style="list-style-type: none"> <li>• Strongly affected by fluorescence</li> <li>• Low sensitivity</li> </ul>	Ocean Insight QE Pro Raman Series Spectrometers - \$15,000 (Ocean Insights, n.d.)  StellarCASE-Raman - \$20,000 (StellarNet Inc, n.d.)

---

LIBS	<ul style="list-style-type: none"> <li>• Applicable to large polymer scope</li> <li>• Able to identify metallic contaminants</li> </ul>	<ul style="list-style-type: none"> <li>• Struggle in distinguishing polymers with similar chemical formula</li> </ul>	StellarCASE-LIBS - \$30,000 (StellarNet Inc, n.d.)
------	---	---	---

---

612 Table 6 shows that there is not an ideal single method for all possible plastic waste fractions  
613 with each having pros and cons. This points to potential benefits of combining different  
614 methods for plastic waste sorting, but this has not been well studied in the literature. In  
615 particular, LIBS and Raman spectroscopy share some synergies in terms of instrumentation,  
616 since both methods involve focusing a laser beam onto the sample, but at different energy  
617 requirements. (Jolivet et al., 2019). Shameem et al., (2017) studied a hybrid LIBS-Raman  
618 system with PE, PP, PET and PS, and found that both methods offer complementary  
619 information. Raman spectroscopy resulted in a clearer separation of different transparent  
620 polymer types but the colored plastic did not form any clear cluster. On the other hand, LIBS  
621 data formed distinct clusters for each of the different plastic types regardless of the color, but  
622 the data were a lot less distinct on a PCA plot. In a related area, Ng et al., (2019) studied the  
623 use of NIR and MIR both separately and in combination for predicting soil properties. The  
624 model built using NIR data was found to perform the worst, while the model built using MIR  
625 data perform at a similar level to the model built using combined NIR and MIR data, which  
626 might point to the redundancy of NIR data in a hybrid system. Therefore, future studies can  
627 focus on performance of hybrid spectroscopic chemometric systems. Developing a unified,  
628 open-sourced database that contains different spectra of the same sample would greatly benefit  
629 exploration of this research direction.

### 630 **7.3 Development of Open-Sourced Database**

631 There are currently existing attempts at building an open-sourced database (Cowger et al., 2021;  
632 Munno et al., 2020). However, in order to realize further developments in the field, namely  
633 expanding of plastic scope and hybrid spectroscopic methods as discussed above, the  
634 information captured in current databases should be expanded, or another standardized open-  
635 sourced database should be developed. This database could contain spectra data of polymers  
636 as a pristine stage, and after simulated aging and contamination (Chabuka and Kalivas, 2020;  
637 Jung et al., 2018; Munno et al., 2020). The difference in spectral features can then be better  
638 captured towards building a chemometric tool for plastic waste sorting that can provide  
639 information on both plastic type and quality. Furthermore, spectra from each of the discussed  
640 spectroscopic methods (NIR, MIR, Raman and LIBS) should be captured for each polymer

641 sample. This allows for potential study to understand whether the use of hybrid spectroscopic  
642 methods can offer better performance in the chemometric analysis. The development of an  
643 open-sourced database can also help to facilitate further exploration of deep learning as  
644 chemometric tool (further discussed in the section below), which relies on large amount of data  
645 for training.

#### 646 **7.4 Deep Learning as Chemometric Tool**

647 Deep learning techniques are considered state-of-the art in many tasks as it allows for learning  
648 of more intricate features as compared to traditional machine learning models (LeCun et al.,  
649 2015). Several works in the literature have explored the use of neural networks as chemometric  
650 tool, but most of the network architectures explored have been basic three-layered ANNs. In  
651 recent years, the field of deep learning has expanded rapidly with different variants of other  
652 neural network architectures like convolutional neural networks (CNN) and recurrent neural  
653 networks (RNN) and generative adversarial networks (GAN) (Wang et al., 2020). In particular,  
654 several works have explored the combination of more novel neural network architectures with  
655 different spectral data in other areas (Chen & Wang, 2019; Liu et al., 2017; Ng et al., 2019,  
656 2020; Peng et al., 2021; Stiebel et al., 2018; Zhang et al., 2019), but only Stiebel et al. (2018)  
657 and Peng et al. (2021) have applied it to plastic sorting. Due to the feature extraction nature of  
658 the network architecture, CNN has been shown to perform well even without any pre-  
659 processing of spectral data (Liu et al., 2017), which reduces the model computation time needed  
660 as compared to other chemometric tools. When applied to classification of the same polymer  
661 LIBS dataset, deep learning models were found to outperform machine learning models like  
662 ANN, SVM and kNN (Peng et al., 2021), which supports the case that the use of deep learning  
663 as chemometric techniques for plastic sorting that should be further explored.

664

665

#### 666 **8. Conclusion**

667 Tackling plastic pollution remains one of the key challenges of the 21<sup>st</sup> century. A lot of  
668 research has been done to help transition the plastic economy to a circular economy, but many  
669 barriers still remain today. In the increasingly digital and fast-moving world, an automated  
670 system built upon chemometrics has shown great potential in helping to boost recycling rates  
671 by improving the sorting process. This review presented a comprehensive overview of the

672 recent works combining the following non-destructive spectroscopic methods - Infrared  
673 spectroscopy, Raman spectroscopy and Laser-induced breakdown spectroscopy with  
674 chemometric tools like principal component analysis, partial least square regression, k-nearest  
675 neighbors, support vector machine and neural networks. Through this review, it can be  
676 concluded that chemometrics combined with non-destructive spectroscopic methods show  
677 good potential in sorting plastics. In an industrial setting, the implementation of chemometrics  
678 have started with near infrared, but the suitability of other spectroscopic methods can be further  
679 tested. The review also reveals that there is potential for further work in this field to derive  
680 further insights from chemical data. Broadly speaking, these include 1) the need to incorporate  
681 other less common polymers or polymers of varying contamination and degradation levels in  
682 training chemometric models, 2) the use of hybrid spectroscopic methods as input data to  
683 overcome the limitations of each of the spectroscopic method, 3) building a standardised  
684 dataset for plastic waste and 4) exploring deep neural networks. By expanding the literature in  
685 these directions, the authors hope that industries will be able to optimize the recycling process  
686 by capturing the maximum value out of plastic waste and transition into a circular economy.

687

688

## 689 **References**

690 Acal Bfi, 2015a. NIR Hyperspectral Imaging System, 950-1700nm or 1200-2200nm [WWW  
691 Document]. URL [https://www.acalbfi.com/uk/Photonics/Spectroscopy/Hyperspectral-](https://www.acalbfi.com/uk/Photonics/Spectroscopy/Hyperspectral-imager/p/NIR-Hyperspectral-Imaging-System--950-1700nm-or-1200-2200nm/0000008KOR)  
692 [imager/p/NIR-Hyperspectral-Imaging-System--950-1700nm-or-1200-](https://www.acalbfi.com/uk/Photonics/Spectroscopy/Hyperspectral-imager/p/NIR-Hyperspectral-Imaging-System--950-1700nm-or-1200-2200nm/0000008KOR)  
693 [2200nm/0000008KOR](https://www.acalbfi.com/uk/Photonics/Spectroscopy/Hyperspectral-imager/p/NIR-Hyperspectral-Imaging-System--950-1700nm-or-1200-2200nm/0000008KOR) (accessed 5.6.21).

694 Acal Bfi, 2015b. MIR Hyperspectral Imaging System, 2900-4200nm [WWW Document].  
695 URL [https://www.acalbfi.com/uk/Photonics/Spectroscopy/Hyperspectral-imager/p/MIR-](https://www.acalbfi.com/uk/Photonics/Spectroscopy/Hyperspectral-imager/p/MIR-Hyperspectral-Imaging-System--2900-4200nm/0000008KOS)  
696 [Hyperspectral-Imaging-System--2900-4200nm/0000008KOS](https://www.acalbfi.com/uk/Photonics/Spectroscopy/Hyperspectral-imager/p/MIR-Hyperspectral-Imaging-System--2900-4200nm/0000008KOS) (accessed 5.6.21).

697 Al-Salem, S.M., Lettieri, P., Baeyens, J., 2009. Recycling and recovery routes of plastic solid  
698 waste (PSW): A review. *Waste Manag.* 29, 2625–2643.  
699 <https://doi.org/https://doi.org/10.1016/j.wasman.2009.06.004>

700 Alassali, A., Fiore, S., Kuchta, K., 2018. Assessment of plastic waste materials degradation  
701 through near infrared spectroscopy. *Waste Manag.* 82, 71–81.

702 <https://doi.org/https://doi.org/10.1016/j.wasman.2018.10.010>

703 Alassali, A., Picuno, C., Bébien, T., Fiore, S., Kuchta, K., 2020. Validation of near infrared  
704 spectroscopy as an age-prediction method for plastics. *Resour. Conserv. Recycl.* 154,  
705 104555. <https://doi.org/https://doi.org/10.1016/j.resconrec.2019.104555>

706 Allen, V., Kalivas, J.H., Rodriguez, R.G., 1999. Post-Consumer Plastic Identification Using  
707 Raman Spectroscopy. *Appl. Spectrosc.* 53, 672–681.

708 Altman, N.S., 1992. An introduction to kernel and nearest-neighbor nonparametric  
709 regression. *Am. Stat.* 46, 175–185.

710 Ángel Aguirre, M., Hidalgo, M., Canals, A., Nóbrega, J.A., Pereira-Filho, E.R., 2013.  
711 Analysis of waste electrical and electronic equipment (WEEE) using laser induced  
712 breakdown spectroscopy (LIBS) and multivariate analysis. *Talanta* 117, 419–424.  
713 <https://doi.org/https://doi.org/10.1016/j.talanta.2013.09.046>

714 Anzano, J., Bonilla, B., Montull-Ibor, B., Lasheras, R., Casas-Gonzalez, J., 2010.  
715 Classifications of Plastic Polymers based on Spectral Data Analysis with laser induced  
716 Breakdown Spectroscopy. *J. Polym. Eng.* 30.  
717 <https://doi.org/10.1515/POLYENG.2010.30.3-4.177>

718 Anzano, J., Lasheras, R.-J., Bonilla, B., Casas, J., 2008. Classification of polymers by  
719 determining of C1:C2:CN:H:N:O ratios by laser-induced plasma spectroscopy (LIPS).  
720 *Polym. Test.* 27, 705–710.  
721 <https://doi.org/https://doi.org/10.1016/j.polymeresting.2008.05.012>

722 Araujo, C.F., Nolasco, M.M., Ribeiro, A.M.P., Ribeiro-Claro, P.J.A., 2018. Identification of  
723 microplastics using Raman spectroscopy: Latest developments and future prospects.  
724 *Water Res.* 142, 426–440. <https://doi.org/https://doi.org/10.1016/j.watres.2018.05.060>

725 Arias, M., Penichet, I., Ysambertt, F., Bauza, R., Zougagh, M., Ríos, Á., 2009. Fast  
726 supercritical fluid extraction of low- and high-density polyethylene additives:  
727 Comparison with conventional reflux and automatic Soxhlet extraction. *J. Supercrit.*  
728 *Fluids* 50, 22–28. <https://doi.org/10.1016/j.supflu.2009.04.012>

729 Bae, J.-S., Oh, S.-K., Pedrycz, W., Fu, Z., 2019. Design of fuzzy radial basis function neural  
730 network classifier based on information data preprocessing for recycling black plastic  
731 wastes: comparative studies of ATR FT-IR and Raman spectroscopy. *Appl. Intell.* 49,

732 929–949. <https://doi.org/10.1007/s10489-018-1300-5>

733 Banaee, M., Tavassoli, S.H., 2012. Discrimination of polymers by laser induced breakdown  
734 spectroscopy together with the DFA method. *Polym. Test.* 31, 759–764.  
735 <https://doi.org/https://doi.org/10.1016/j.polymertesting.2012.04.010>

736 Baskaran, S., Sathiavelu, M., 2020. Application of Attenuated Total Reflection - Fourier  
737 Transform Infrared spectroscopy to characterize the degradation of littered multilayer  
738 food packaging plastics. *Vib. Spectrosc.* 109, 103105.  
739 <https://doi.org/https://doi.org/10.1016/j.vibspec.2020.103105>

740 Becker, W., Sachsenheimer, K., Klemenz, M., 2017. Detection of Black Plastics in the  
741 Middle Infrared Spectrum (MIR) Using Photon Up-Conversion Technique for Polymer  
742 Recycling Purposes. *Polym.* . <https://doi.org/10.3390/polym9090435>

743 Beigbeder, J., Perrin, D., Mascaro, J.-F., Lopez-Cuesta, J.-M., 2013. Study of the physico-  
744 chemical properties of recycled polymers from waste electrical and electronic equipment  
745 (WEEE) sorted by high resolution near infrared devices. *Resour. Conserv. Recycl.* 78,  
746 105–114. <https://doi.org/https://doi.org/10.1016/j.resconrec.2013.07.006>

747 Biancolillo, A., Marini, F., 2018. Chemometric Methods for Spectroscopy-Based  
748 Pharmaceutical Analysis . *Front. Chem.* .

749 Bonifazi, G., Fiore, L., Hennebert, P., Serranti, S., 2020. An Efficient Strategy Based on  
750 Hyperspectral Imaging for Brominated Plastic Waste Sorting in a Circular Economy  
751 Perspective BT - *Advances in Polymer Processing 2020*, in: Hopmann, C., Dahlmann,  
752 R. (Eds.), . Springer Berlin Heidelberg, Berlin, Heidelberg, pp. 14–27.

753 Bonifazi, G., Gasbarrone, R., Serranti, S., 2021. Detecting Contaminants in Post-Consumer  
754 Plastic Packaging Waste by a NIR Hyperspectral Imaging-based Cascade Detection  
755 Approach. *Detritus.* <https://doi.org/10.31025/2611-4135/2021.14086>

756 Bonifazi, G., Maio, F. Di, Potenza, F., Serranti, S., 2014. FT-IR spectroscopy and  
757 Hyperspectral Imaging applied to post-consumer plastic packaging characterization and  
758 sorting, in: *SENSORS, 2014 IEEE.* pp. 633–636.  
759 <https://doi.org/10.1109/ICSENS.2014.6985078>

760 Boueri, M., Motto-Ros, V., Lei, W.-Q., Qain-LiMa, Zheng, L.-J., Zeng, H.-P., JinYu, 2011.  
761 Identification of Polymer Materials Using Laser-Induced Breakdown Spectroscopy



762 Combined with Artificial Neural Networks. *Appl. Spectrosc.* 65, 307–314.

763 Breiman, L., 2001. Random Forests. *Mach. Learn.* 45, 5–32.

764 <https://doi.org/10.1023/A:1010933404324>

765 Brouwer, M.T., Alvarado Chacon, F., Thoden van Velzen, E.U., 2020. Effect of recycled  
766 content and rPET quality on the properties of PET bottles, part III: Modelling of  
767 repetitive recycling. *Packag. Technol. Sci.* 33, 373–383.

768 <https://doi.org/https://doi.org/10.1002/pts.2489>

769 Caballero, D., Bevilacqua, M., Amigo, J., 2019. Application of hyperspectral imaging and  
770 chemometrics for classifying plastics with brominated flame retardants. *J. Spectr.*  
771 *Imaging* 8. <https://doi.org/10.1255/jsi.2019.a1>

772 Cabanes, A., Valdés, F.J., Fullana, A., 2020. A review on VOCs from recycled plastics.  
773 *Sustain. Mater. Technol.* 25, e00179.

774 <https://doi.org/https://doi.org/10.1016/j.susmat.2020.e00179>

775 Calvini, R., Orlandi, G., Foca, G., Ulrici, A., 2018. Development of a classification algorithm  
776 for efficient handling of multiple classes in sorting systems based on hyperspectral  
777 imaging. *J. Spectr. Imaging* 7. <https://doi.org/10.1255/jsi.2018.a13>

778 Campanale, C., Massarelli, C., Savino, I., Locaputo, V., Uricchio, V.F., 2020. A Detailed  
779 Review Study on Potential Effects of Microplastics and Additives of Concern on Human  
780 Health. *Int. J. Environ. Res. Public Health* 17, 1212.

781 <https://doi.org/10.3390/ijerph17041212>

782 Canopoli, L., Coulon, F., Wagland, S.T., 2020. Degradation of excavated polyethylene and  
783 polypropylene waste from landfill. *Sci. Total Environ.* 698, 134125.

784 <https://doi.org/https://doi.org/10.1016/j.scitotenv.2019.134125>

785 Chabuka, B.K., Kalivas, J.H., 2020. Application of a Hybrid Fusion Classification Process  
786 for Identification of Microplastics Based on Fourier Transform Infrared Spectroscopy.  
787 *Appl. Spectrosc.* 74, 1167–1183.

788 Chapman, J., Truong, V.K., Elbourne, A., Gangadoo, S., Cheeseman, S., Rajapaksha, P.,  
789 Latham, K., Crawford, R.J., Cozzolino, D., 2020. Combining Chemometrics and  
790 Sensors: Toward New Applications in Monitoring and Environmental Analysis. *Chem.*  
791 *Rev.* 120, 6048–6069. <https://doi.org/10.1021/acs.chemrev.9b00616>

- 792 Chen, L., Jin, S., Li, W., 2017. Rapid identification of plastics based on Raman spectroscopy  
793 with the combination of support vector machine, in: 2017 16th International Conference  
794 on Optical Communications and Networks (ICO CN). pp. 1–3.  
795 <https://doi.org/10.1109/ICO CN.2017.8121214>
- 796 Chen, X., Kroell, N., Dietl, T., Feil, A., Greiff, K., 2021a. Influence of long-term natural  
797 degradation processes on near-infrared spectra and sorting of post-consumer plastics.  
798 *Waste Manag.* 136, 213–218.  
799 <https://doi.org/https://doi.org/10.1016/j.wasman.2021.10.006>
- 800 Chen, X., Kroell, N., Wickel, J., Feil, A., 2021b. Determining the composition of post-  
801 consumer flexible multilayer plastic packaging with near-infrared spectroscopy. *Waste*  
802 *Manag.* 123, 33–41. <https://doi.org/https://doi.org/10.1016/j.wasman.2021.01.015>
- 803 Chen, Y.-Y., Wang, Z.-B., 2019. End-to-end quantitative analysis modeling of near-infrared  
804 spectroscopy based on convolutional neural network. *J. Chemom.* 33, e3122.  
805 <https://doi.org/https://doi.org/10.1002/cem.3122>
- 806 Costa, V.C., Aquino, F.W.B., Paranhos, C.M., Pereira-Filho, E.R., 2017. Identification and  
807 classification of polymer e-waste using laser-induced breakdown spectroscopy (LIBS)  
808 and chemometric tools. *Polym. Test.* 59, 390–395.  
809 <https://doi.org/https://doi.org/10.1016/j.polymertesting.2017.02.017>
- 810 Costa, V.C., Pereira, F.M.V., 2020. Laser-induced breakdown spectroscopy applied to the  
811 rapid identification of different types of polyethylene used for toy manufacturing. *J.*  
812 *Chemom.* 34, e3248. <https://doi.org/https://doi.org/10.1002/cem.3248>
- 813 Cowger, W., Steinmetz, Z., Gray, A., Munno, K., Lynch, J., Hapich, H., Primpke, S., De  
814 Frond, H., Rochman, C., Herodotou, O., 2021. Microplastic Spectral Classification  
815 Needs an Open Source Community: Open Specy to the Rescue! *Anal. Chem.* 93, 7543–  
816 7548. <https://doi.org/10.1021/acs.analchem.1c00123>
- 817 da Silva, D.J., Wiebeck, H., 2020. Current options for characterizing, sorting, and recycling  
818 polymeric waste. *Prog. Rubber, Plast. Recycl. Technol.* 36, 284–303.  
819 <https://doi.org/10.1177/1477760620918603>
- 820 De Biasio, M., Arnold, T., Mcgunnigle, G., Leitner, R., Balthasar, D., Rehrmann, V., 2010.  
821 Detecting and Discriminating PE and PP Polymers for Plastics Recycling Using NIR

822 Imaging Spectroscopy 7661. <https://doi.org/10.1117/12.850065>

823 Dodbiba, G., Fujita, T., 2004. Progress in Separating Plastic Materials for Recycling. *Phys.*  
824 *Sep. Sci. Eng.* 13, 594923. <https://doi.org/10.1080/14786470412331326350>

825 Dong, M., Zhang, Q., Xing, X., Chen, W., She, Z., Luo, Z., 2020. Raman spectra and surface  
826 changes of microplastics weathered under natural environments. *Sci. Total Environ.* 739,  
827 139990. <https://doi.org/10.1016/j.scitotenv.2020.139990>

828 Ellen MacArthur Foundation, 2017. *The New Plastics Economy - Rethinking the Future of*  
829 *PLastics.*

830 Feldhoff, R., Huth-Fehre, T., Kantimm, T., Quick, L., Cammann, K., van den Broek, W.,  
831 Wienke, D., Fuchs, H., 1995. Fast Identification of Packaging Waste by near Infrared  
832 Spectroscopy with an InGaAs Array Spectrograph Combined with Neural Networks. *J.*  
833 *Near Infrared Spectrosc.* 3, 3–9.

834 Feldhoff, R., Wienke, D., Cammann, K., Fuchs, H., 1997. On-Line Post Consumer Package  
835 Identification by NIR Spectroscopy Combined with a FuzzyARTMAP Classifier in an  
836 Industrial Environment. *Appl. Spectrosc.* 51, 362–368.  
837 <https://doi.org/10.1366/0003702971940215>

838 Ferronato, N., Torretta, V., 2019. Waste Mismanagement in Developing Countries: A Review  
839 of Global Issues. *Int. J. Environ. Res. Public Health* 16, 1060.  
840 <https://doi.org/10.3390/ijerph16061060>

841 Florestan, J., Lachambre, A., Mermilliod, N., Boulou, J.C., Marfisi, C., 1994. Recycling of  
842 plastics: Automatic identification of polymers by spectroscopic methods. *Resour.*  
843 *Conserv. Recycl.* 10, 67–74. [https://doi.org/https://doi.org/10.1016/0921-](https://doi.org/https://doi.org/10.1016/0921-3449(94)90039-6)  
844 [3449\(94\)90039-6](https://doi.org/https://doi.org/10.1016/0921-3449(94)90039-6)

845 Gabriel, D.S., Maulana, J., 2018. Impact of Plastic Labelling, Coloring and Printing on  
846 Material Value Conservation in the Products of Secondary Recycling. *Key Eng. Mater.*  
847 773, 384–389. <https://doi.org/10.4028/www.scientific.net/KEM.773.384>

848 Galdón-Navarro, B., Prats-Montalbán, J.M., Cubero, S., Blasco, J., Ferrer, A., 2018.  
849 Comparison of latent variable-based and artificial intelligence methods for impurity  
850 detection in PET recycling from NIR hyperspectral images. *J. Chemom.* 32, e2980.  
851 <https://doi.org/https://doi.org/10.1002/cem.2980>

852 Geyer, R., Jambeck, J.R., Law, K.L., 2017. Production, use, and fate of all plastics ever  
853 made. *Sci. Adv.* 3, e1700782. <https://doi.org/10.1126/sciadv.1700782>

854 Godoi, Q., Leme, F.O., Trevizan, L.C., Pereira Filho, E.R., Rufini, I.A., Santos, D., Krug,  
855 F.J., 2011. Laser-induced breakdown spectroscopy and chemometrics for classification  
856 of toys relying on toxic elements. *Spectrochim. Acta Part B At. Spectrosc.* 66, 138–143.  
857 <https://doi.org/https://doi.org/10.1016/j.sab.2011.01.001>

858 Gondal, M.A., Siddiqui, M.N., 2007. Identification of different kinds of plastics using laser-  
859 induced breakdown spectroscopy for waste management. *J. Environ. Sci. Heal. Part A*  
860 42, 1989–1997. <https://doi.org/10.1080/10934520701628973>

861 Grégoire, S., Boudinet, M., Pelascini, F., Surma, F., Detalle, V., Holl, Y., 2011. Laser-  
862 induced breakdown spectroscopy for polymer identification. *Anal. Bioanal. Chem.* 400,  
863 3331–3340. <https://doi.org/10.1007/s00216-011-4898-2>

864 Griffiths, P.R., De Haseth, J.A., Winefordner, J.D., 2007. *Fourier Transform Infrared*  
865 *Spectrometry, Chemical Analysis: A Series of Monographs on Analytical Chemistry and*  
866 *Its Applications.* Wiley.

867 Gundupalli, S.P., Hait, S., Thakur, A., 2017. A review on automated sorting of source-  
868 separated municipal solid waste for recycling. *Waste Manag.* 60, 56–74.  
869 <https://doi.org/https://doi.org/10.1016/j.wasman.2016.09.015>

870 Guo, Y., Tang, Y., Du, Y., Tang, S., Guo, L., Li, X., Lu, Y., Zeng, X., 2018. Cluster analysis  
871 of polymers using laser-induced breakdown spectroscopy with K-means. *Plasma Sci.*  
872 *Technol.* 20, 65505. <https://doi.org/10.1088/2058-6272/aaaade>

873 Haenlein, M., Kaplan, A.M., 2004. *A Beginner's Guide to Partial Least Squares Analysis.*  
874 *Underst. Stat.* 3, 283–297. [https://doi.org/10.1207/s15328031us0304\\_4](https://doi.org/10.1207/s15328031us0304_4)

875 Heberger, Karoly, 2008. Chapter 7 - Chemoinformatics—multivariate mathematical—  
876 statistical methods for data evaluation, in: Vékey, K., Telekes, A., Vertes, A.B.T.-M.A.  
877 of M.S. (Eds.), . Elsevier, Amsterdam, pp. 141–169.  
878 <https://doi.org/https://doi.org/10.1016/B978-044451980-1.50009-4>

879 Hopewell, J., Dvorak, R., Kosior, E., 2009. Plastics recycling: challenges and opportunities.  
880 *Philos. Trans. R. Soc. B Biol. Sci.* 364, 2115–2126.

881 Huber, N., Eschlböck-Fuchs, S., Scherndl, H., Freimund, A., Heitz, J., Pedarnig, J.D., 2014.

882 In-line measurements of chlorine containing polymers in an industrial waste sorting  
883 plant by laser-induced breakdown spectroscopy. *Appl. Surf. Sci.* 302, 280–285.  
884 <https://doi.org/https://doi.org/10.1016/j.apsusc.2013.10.070>

885 Huth-Fehre, T., Feldhoff, R., Kantimm, T., Quick, L., Winter, F., Cammann, K., van den  
886 Broek, W., Wienke, D., Melssen, W., Buydens, L., 1995. NIR - Remote sensing and  
887 artificial neural networks for rapid identification of post consumer plastics. *J. Mol.*  
888 *Struct.* 348, 143–146. [https://doi.org/https://doi.org/10.1016/0022-2860\(95\)08609-Y](https://doi.org/https://doi.org/10.1016/0022-2860(95)08609-Y)

889 Izenman, Alan Julian, 2008. *Linear Discriminant Analysis BT - Modern Multivariate*  
890 *Statistical Techniques: Regression, Classification, and Manifold Learning*, in: Izenman,  
891 Alan J (Ed.), . Springer New York, New York, NY, pp. 237–280.  
892 [https://doi.org/10.1007/978-0-387-78189-1\\_8](https://doi.org/10.1007/978-0-387-78189-1_8)

893 Jacquin, L., Imoussaten, A., Troussset, F., Perrin, D., Montmain, J., 2021. Control of waste  
894 fragment sorting process based on MIR imaging coupled with cautious classification.  
895 *Resour. Conserv. Recycl.* 168, 105258.  
896 <https://doi.org/https://doi.org/10.1016/j.resconrec.2020.105258>

897 Jambeck, J.R., Geyer, R., Wilcox, C., Siegler, T.R., Perryman, M., Andrady, A., Narayan, R.,  
898 Law, K.L., 2015. Plastic waste inputs from land into the ocean. *Science* (80-. ). 347,  
899 768–771.

900 Jolivet, L., Leprince, M., Moncayo, S., Sorbier, L., Lienemann, C.-P., Motto-Ros, V., 2019.  
901 Review of the recent advances and applications of LIBS-based imaging. *Spectrochim.*  
902 *Acta Part B At. Spectrosc.* 151, 41–53.  
903 <https://doi.org/https://doi.org/10.1016/j.sab.2018.11.008>

904 Jolliffe, I.T., Cadima, J., 2016. Principal component analysis: a review and recent  
905 developments. *Philos. Trans. R. Soc. A Math. Phys. Eng. Sci.* 374, 20150202.  
906 <https://doi.org/10.1098/rsta.2015.0202>

907 Jung, M.R., Horgen, F.D., Orski, S. V, Rodriguez C., V., Beers, K.L., Balazs, G.H., Jones,  
908 T.T., Work, T.M., Brignac, K.C., Royer, S.-J., Hyrenbach, K.D., Jensen, B.A., Lynch,  
909 J.M., 2018. Validation of ATR FT-IR to identify polymers of plastic marine debris,  
910 including those ingested by marine organisms. *Mar. Pollut. Bull.* 127, 704–716.  
911 <https://doi.org/https://doi.org/10.1016/j.marpolbul.2017.12.061>

912 Junjuri, R., Gundawar, M.K., 2020. A low-cost LIBS detection system combined with  
913 chemometrics for rapid identification of plastic waste. *Waste Manag.* 117, 48–57.  
914 <https://doi.org/https://doi.org/10.1016/j.wasman.2020.07.046>

915 Junjuri, R., Gundawar, M.K., 2019. Femtosecond laser-induced breakdown spectroscopy  
916 studies for the identification of plastics. *J. Anal. At. Spectrom.* 34, 1683–1692.  
917 <https://doi.org/10.1039/C9JA00102F>

918 Junjuri, R., Zhang, C., Barman, I., Gundawar, M.K., 2019. Identification of post-consumer  
919 plastics using laser-induced breakdown spectroscopy. *Polym. Test.* 76, 101–108.  
920 <https://doi.org/https://doi.org/10.1016/j.polymertesting.2019.03.012>

921 Karaca, A.C., Ertürk, A., Güllü, M.K., Elmas, M., Ertürk, S., 2013. Automatic waste sorting  
922 using shortwave infrared hyperspectral imaging system, in: 2013 5th Workshop on  
923 Hyperspectral Image and Signal Processing: Evolution in Remote Sensing  
924 (WHISPERS). pp. 1–4. <https://doi.org/10.1109/WHISPERS.2013.8080744>

925 Kassouf, A., Maalouly, J., Rutledge, D.N., Chebib, H., Ducruet, V., 2014. Rapid  
926 discrimination of plastic packaging materials using MIR spectroscopy coupled with  
927 independent components analysis (ICA). *Waste Manag.* 34, 2131–2138.  
928 <https://doi.org/https://doi.org/10.1016/j.wasman.2014.06.015>

929 Kempfert, K.D., Jiang, E.Y., Oas, S., Coffin, J., 2001. Detectors for Fourier transform  
930 spectroscopy. AN-00125.

931 Kim, H., Kim, S., 2016. Band selection for plastic classification using NIR hyperspectral  
932 image, in: 2016 16th International Conference on Control, Automation and Systems  
933 (ICCAS). pp. 302–304. <https://doi.org/10.1109/ICCAS.2016.7832335>

934 Krenker, A., Bešter, J., Kos, A., 2011. Introduction to the artificial neural networks. *Artif.*  
935 *Neural Networks Methodol. Adv. Biomed. Appl. InTech* 1–18.

936 LeCun, Y., Bengio, Y., Hinton, G., 2015. Deep learning. *Nature* 521, 436–444.  
937 <https://doi.org/10.1038/nature14539>

938 Lecun, Y., Bottou, L., Bengio, Y., Haffner, P., 1998. Gradient-based learning applied to  
939 document recognition. *Proc. IEEE* 86, 2278–2324. <https://doi.org/10.1109/5.726791>

940 Lee, Y., Lin, Y., Wahba, G., 2004. Multicategory Support Vector Machines. *J. Am. Stat.*  
941 *Assoc.* 99, 67–81. <https://doi.org/10.1198/016214504000000098>

- 942 Liang, N., Sun, S., Zhang, C., He, Y., Qiu, Z., 2020. Advances in infrared spectroscopy  
943 combined with artificial neural network for the authentication and traceability of food.  
944 *Crit. Rev. Food Sci. Nutr.* 1–22. <https://doi.org/10.1080/10408398.2020.1862045>
- 945 Likas, A., Vlassis, N., J. Verbeek, J., 2003. The global k-means clustering algorithm. *Pattern*  
946 *Recognit.* 36, 451–461. [https://doi.org/https://doi.org/10.1016/S0031-3203\(02\)00060-2](https://doi.org/https://doi.org/10.1016/S0031-3203(02)00060-2)
- 947 Liu, J., Osadchy, M., Ashton, L., Foster, M., Solomon, C.J., Gibson, S.J., 2017. Deep  
948 convolutional neural networks for Raman spectrum recognition: a unified solution.  
949 *Analyst* 142, 4067–4074. <https://doi.org/10.1039/C7AN01371J>
- 950 Liu, K., Tian, D., Li, C., Li, Y., Yang, G., Ding, Y., 2019a. A review of laser-induced  
951 breakdown spectroscopy for plastic analysis. *TrAC Trends Anal. Chem.* 110, 327–334.  
952 <https://doi.org/https://doi.org/10.1016/j.trac.2018.11.025>
- 953 Liu, K., Tian, D., Wang, H., Yang, G., 2019b. Rapid classification of plastics by laser-  
954 induced breakdown spectroscopy (LIBS) coupled with partial least squares  
955 discrimination analysis based on variable importance (VI-PLS-DA). *Anal. Methods* 11,  
956 1174–1179. <https://doi.org/10.1039/C8AY02755B>
- 957 Liu, K., Tian, D., Xu, H., Wang, H., Yang, G., 2019c. Quantitative analysis of toxic elements  
958 in polypropylene (PP) via laser-induced breakdown spectroscopy (LIBS) coupled with  
959 random forest regression based on variable importance (VI-RFR). *Anal. Methods* 11,  
960 4769–4774. <https://doi.org/10.1039/C9AY01796H>
- 961 LLA Instruments, n.d. Hyperspectral NIR Cameras [WWW Document]. URL  
962 <https://www.lla-instruments.com/files/lla/pdf/Geraetetechnik>  
963 [ENG/KUSTA1.7MSI\\_KUSTA1.9MSI\\_KUSTA2.2MSI.pdf](https://www.lla-instruments.com/files/lla/pdf/Geraetetechnik) (accessed 5.6.21).
- 964 Malcolm Richard, G., Mario, M., Javier, T., Susana, T., 2011. Optimization of the recovery  
965 of plastics for recycling by density media separation cyclones. *Resour. Conserv. Recycl.*  
966 55, 472–482. <https://doi.org/https://doi.org/10.1016/j.resconrec.2010.12.010>
- 967 Marica, A.I., Aluaş, M., Pînzaru, S.C., 2019. The Management and Stewardship of Medical  
968 Plastic Waste using Raman Spectroscopy to Sustain Circular Economy, in: 2019 E-  
969 Health and Bioengineering Conference (EHB). pp. 1–4.  
970 <https://doi.org/10.1109/EHB47216.2019.8970076>
- 971 McCreery, R.L., 2005. Raman Spectroscopy for Chemical Analysis, *Chemical Analysis: A*

972 Series of Monographs on Analytical Chemistry and Its Applications. Wiley.

973 Milios, L., Holm Christensen, L., McKinnon, D., Christensen, C., Rasch, M.K., Hallstrøm  
974 Eriksen, M., 2018. Plastic recycling in the Nordics: A value chain market analysis.  
975 Waste Manag. 76, 180–189.  
976 <https://doi.org/https://doi.org/10.1016/j.wasman.2018.03.034>

977 Munno, K., De Frond, H., O'Donnell, B., Rochman, C.M., 2020. Increasing the Accessibility  
978 for Characterizing Microplastics: Introducing New Application-Based and Spectral  
979 Libraries of Plastic Particles (SLoPP and SLoPP-E). Anal. Chem. 92, 2443–2451.  
980 <https://doi.org/10.1021/acs.analchem.9b03626>

981 Musu, W., Tsuchida, A., Kawazumi, H., Oka, N., 2019. Application of PCA-SVM and ANN  
982 Techniques for Plastic Identification by Raman Spectroscopy, in: 2019 1st International  
983 Conference on Cybernetics and Intelligent System (ICORIS). pp. 114–118.  
984 <https://doi.org/10.1109/ICORIS.2019.8874880>

985 Mylläri, V., Hartikainen, S., Poliakova, V., Anderson, R., Jönkkäri, I., Pasanen, P.,  
986 Andersson, M., Vuorinen, J., 2016. Detergent impurity effect on recycled HDPE:  
987 Properties after repetitive processing. J. Appl. Polym. Sci. 133, 1–8.  
988 <https://doi.org/10.1002/app.43766>

989 Ng, W., Minasny, B., McBratney, A., 2020. Convolutional neural network for soil  
990 microplastic contamination screening using infrared spectroscopy. Sci. Total Environ.  
991 702, 134723. <https://doi.org/https://doi.org/10.1016/j.scitotenv.2019.134723>

992 Ng, W., Minasny, B., Montazerolghaem, M., Padarian, J., Ferguson, R., Bailey, S.,  
993 McBratney, A.B., 2019. Convolutional neural network for simultaneous prediction of  
994 several soil properties using visible/near-infrared, mid-infrared, and their combined  
995 spectra. Geoderma 352, 251–267.  
996 <https://doi.org/https://doi.org/10.1016/j.geoderma.2019.06.016>

997 Ocean Insights, n.d. Spectrometers | Ocean Insight [WWW Document]. URL  
998 <https://www.oceaninsight.com/products/spectrometers/> (accessed 5.25.21).

999 OECD, 2018. Improving Plastics Management: Trends, policy responses, and the role of  
1000 international co-operation and trade.

1001 Pasquini, C., 2018. Near infrared spectroscopy: A mature analytical technique with new



1002 perspectives – A review. *Anal. Chim. Acta* 1026, 8–36.  
1003 <https://doi.org/https://doi.org/10.1016/j.aca.2018.04.004>

1004 Pelegrini, K., Maraschin, T.G., Brandalise, R.N., Piazza, D., 2019. Study of the degradation  
1005 and recyclability of polyethylene and polypropylene present in the marine environment.  
1006 *J. Appl. Polym. Sci.* 136, 48215. <https://doi.org/https://doi.org/10.1002/app.48215>

1007 Peng, X., Xu, B., Xu, Z., Yan, X., Zhang, N., Qin, Y., Ma, Q., Li, J., Zhao, N., Zhang, Q.,  
1008 2021. Accuracy improvement in plastics classification by laser-induced breakdown  
1009 spectroscopy based on a residual network. *Opt. Express* 29, 33269–33280.  
1010 <https://doi.org/10.1364/OE.438331>

1011 Pieszczek, L., Daszykowski, M., 2019. Improvement of recyclable plastic waste detection –  
1012 A novel strategy for the construction of rigorous classifiers based on the hyperspectral  
1013 images. *Chemom. Intell. Lab. Syst.* 187, 28–40.  
1014 <https://doi.org/https://doi.org/10.1016/j.chemolab.2019.02.009>

1015 Primpke, S., Christiansen, S.H., Cowger, W., De Frond, H., Deshpande, A., Fischer, M.,  
1016 Holland, E.B., Meyns, M., O'Donnell, B.A., Ossmann, B.E., Pittroff, M., Sarau, G.,  
1017 Scholz-Böttcher, B.M., Wiggin, K.J., 2020. Critical Assessment of Analytical Methods  
1018 for the Harmonized and Cost-Efficient Analysis of Microplastics. *Appl. Spectrosc.* 74,  
1019 1012–1047. <https://doi.org/10.1177/0003702820921465>

1020 Ragusa, A., Svelato, A., Santacroce, C., Catalano, P., Notarstefano, V., Carnevali, O., Papa,  
1021 F., Rongioletti, M.C.A., Baiocco, F., Draghi, S., D'Amore, E., Rinaldo, D., Matta, M.,  
1022 Giorgini, E., 2021. Plasticenta: First evidence of microplastics in human placenta.  
1023 *Environ. Int.* 146, 106274. <https://doi.org/https://doi.org/10.1016/j.envint.2020.106274>

1024 Rani, M., Marchesi, C., Federici, S., Rovelli, G., Alessandri, I., Vassalini, I., Ducoli, S.,  
1025 Borgese, L., Zacco, A., Bilo, F., Bontempi, E., Depero, L.E., 2019. Miniaturized Near-  
1026 Infrared (MicroNIR) Spectrometer in Plastic Waste Sorting. *Mater.* .  
1027 <https://doi.org/10.3390/ma12172740>

1028 Resonon, 2020. Hyperspectral Imaging Cameras [WWW Document]. URL  
1029 [https://photonlines.co.uk/wp-content/uploads/2020/08/Resonon-Hyperspectral-Imaging-](https://photonlines.co.uk/wp-content/uploads/2020/08/Resonon-Hyperspectral-Imaging-Cameras.pdf)  
1030 [Cameras.pdf](https://photonlines.co.uk/wp-content/uploads/2020/08/Resonon-Hyperspectral-Imaging-Cameras.pdf) (accessed 5.6.21).

1031 Ritchie, H., 2018. Plastic Pollution. Our World Data.

- 1032 Roh, S.-B., Oh, S.-K., Park, E.-K., Choi, W.Z., 2017. Identification of black plastics realized  
1033 with the aid of Raman spectroscopy and fuzzy radial basis function neural networks  
1034 classifier. *J. Mater. Cycles Waste Manag.* 19, 1093–1105.  
1035 <https://doi.org/10.1007/s10163-017-0620-6>
- 1036 Roh, S.-B., Park, S.-B., Oh, S.-K., Park, E.-K., Choi, W.Z., 2018. Development of intelligent  
1037 sorting system realized with the aid of laser-induced breakdown spectroscopy and  
1038 hybrid preprocessing algorithm-based radial basis function neural networks for recycling  
1039 black plastic wastes. *J. Mater. Cycles Waste Manag.* 20, 1934–1949.  
1040 <https://doi.org/10.1007/s10163-018-0701-1>
- 1041 Ruj, B., Pandey, V., Jash, P., Srivastava, V., 2015. Sorting of plastic waste for effective  
1042 recycling. *Int. J. Appl. Sci. Eng. Res.* 4. <https://doi.org/10.6088/ijaser.04058>
- 1043 Saeki, K., Tanabe, K., Matsumoto, T., Uesaka, H., Amano, T., Funatsu, K., 2003. Prediction  
1044 of Polyethylene Density by Near-Infrared Spectroscopy Combined with Neural Network  
1045 Analysis. *J. Comput. Chem. Jpn* 2, 33–40. <https://doi.org/10.2477/jccj.2.33>
- 1046 Said, M., Amr, M., Sabry, Y., Khalil, D., Wahba, A., 2020. Plastic sorting based on MEMS  
1047 FTIR spectral chemometrics sensing, in: *Proc.SPIE*.
- 1048 Sato, H., Shimoyama, M., Kamiya, T., Amari, T., Šašić, S., Ninomiya, T., Siesler, H.W.,  
1049 Ozaki, Y., 2002. Raman spectra of high-density, low-density, and linear low-density  
1050 polyethylene pellets and prediction of their physical properties by multivariate data  
1051 analysis. *J. Appl. Polym. Sci.* 86, 443–448.  
1052 <https://doi.org/https://doi.org/10.1002/app.10999>
- 1053 Sauzier, G., van Bronswijk, W., Lewis, S.W., 2021. Chemometrics in forensic science:  
1054 approaches and applications. *Analyst* 146, 2415–2448.  
1055 <https://doi.org/10.1039/D1AN00082A>
- 1056 Serranti, S., Cucuzza, P., Bonifazi, G., 2020. Hyperspectral imaging for VIS-SWIR  
1057 classification of post-consumer plastic packaging products by polymer and color, in:  
1058 *Proc.SPIE*.
- 1059 Serranti, S., Gargiulo, A., Bonifazi, G., 2012. Hyperspectral Imaging for Process and Quality  
1060 Control in Recycling Plants of Polyolefin Flakes. *J. Near Infrared Spectrosc.* 20, 573–  
1061 581. <https://doi.org/10.1255/jnirs.1016>

1062 Serranti, S., Gargiulo, A., Bonifazi, G., 2011. Characterization of post-consumer polyolefin  
1063 wastes by hyperspectral imaging for quality control in recycling processes. *Waste*  
1064 *Manag.* 31, 2217–2227. <https://doi.org/https://doi.org/10.1016/j.wasman.2011.06.007>

1065 Serranti, S., Luciani, V., Bonifazi, G., Hu, B., Rem, P.C., 2015. An innovative recycling  
1066 process to obtain pure polyethylene and polypropylene from household waste. *Waste*  
1067 *Manag.* 35, 12–20. <https://doi.org/https://doi.org/10.1016/j.wasman.2014.10.017>

1068 Shameem, K.M.M., Choudhari, K.S., Bankapur, A., Kulkarni, S.D., Unnikrishnan, V.K.,  
1069 George, S.D., Kartha, V.B., Santhosh, C., 2017. A hybrid LIBS–Raman system  
1070 combined with chemometrics: an efficient tool for plastic identification and sorting.  
1071 *Anal. Bioanal. Chem.* 409, 3299–3308. <https://doi.org/10.1007/s00216-017-0268-z>

1072 Signoret, C., Caro-Bretelle, A.-S., Lopez-Cuesta, J.-M., Ienny, P., Perrin, D., 2020.  
1073 Alterations of plastics spectra in MIR and the potential impacts on identification towards  
1074 recycling. *Resour. Conserv. Recycl.* 161, 104980.  
1075 <https://doi.org/https://doi.org/10.1016/j.resconrec.2020.104980>

1076 Signoret, C., Caro-Bretelle, A.-S., Lopez-Cuesta, J.-M., Ienny, P., Perrin, D., 2019a. MIR  
1077 spectral characterization of plastic to enable discrimination in an industrial recycling  
1078 context: I. Specific case of styrenic polymers. *Waste Manag.* 95, 513–525.  
1079 <https://doi.org/https://doi.org/10.1016/j.wasman.2019.05.050>

1080 Signoret, C., Caro-Bretelle, A.-S., Lopez-Cuesta, J.-M., Ienny, P., Perrin, D., 2019b. MIR  
1081 spectral characterization of plastic to enable discrimination in an industrial recycling  
1082 context: II. Specific case of polyolefins. *Waste Manag.* 98, 160–172.  
1083 <https://doi.org/https://doi.org/10.1016/j.wasman.2019.08.010>

1084 Silva, D.J. da, Wiebeck, H., 2019. Predicting LDPE/HDPE blend composition by CARS-PLS  
1085 regression and confocal Raman spectroscopy . *Polímeros* .

1086 Singh, J.P., Thakur, S., 2020. *Laser-Induced Breakdown Spectroscopy*. Elsevier Science.

1087 Smith, L.I., 2002. A tutorial on principal components analysis.

1088 Specim, 2020a. Specim FX17 [WWW Document]. URL [https://www.specim.fi/wp-](https://www.specim.fi/wp-content/uploads/2020/03/Specim-FX17-Technical-Datasheet-02.pdf)  
1089 [content/uploads/2020/03/Specim-FX17-Technical-Datasheet-02.pdf](https://www.specim.fi/wp-content/uploads/2020/03/Specim-FX17-Technical-Datasheet-02.pdf) (accessed 5.6.21).

1090 Specim, 2020b. Specim FX50 [WWW Document]. URL [https://www.specim.fi/wp-](https://www.specim.fi/wp-content/uploads/2020/03/Specim-FX50-Technical-Datasheet-02.pdf)  
1091 [content/uploads/2020/03/Specim-FX50-Technical-Datasheet-02.pdf](https://www.specim.fi/wp-content/uploads/2020/03/Specim-FX50-Technical-Datasheet-02.pdf) (accessed 5.6.21).

- 1092 Stefan, D., Gyftokostas, N., Bellou, E., Couris, S., 2019. Laser-Induced Breakdown  
1093 Spectroscopy Assisted by Machine Learning for Plastics/Polymers Identification.  
1094 *Atoms* . <https://doi.org/10.3390/atoms7030079>
- 1095 StellarNet Inc, n.d. Online Quotation Generator [WWW Document]. URL  
1096 <https://www.stellarnet.us/online-quotation-generator/> (accessed 5.25.21).
- 1097 Stiebel, T., Bosling, M., Steffens, A., Pretz, T., Merhof, D., 2018. An Inspection System for  
1098 Multi-Label Polymer Classification, in: 2018 IEEE 23rd International Conference on  
1099 Emerging Technologies and Factory Automation (ETFA). pp. 623–630.  
1100 <https://doi.org/10.1109/ETFA.2018.8502474>
- 1101 Strangl, M., Lok, B., Breunig, P., Ortner, E., Buettner, A., 2021. The challenge of  
1102 deodorizing post-consumer polypropylene packaging: Screening of the effect of  
1103 washing, color-sorting and heat exposure. *Resour. Conserv. Recycl.* 164, 105143.  
1104 <https://doi.org/10.1016/j.resconrec.2020.105143>
- 1105 Stuart, M.B., Stanger, L.R., Hobbs, M.J., Pering, T.D., Thio, D., McGonigle, A.J.S.,  
1106 Willmott, J.R., 2020. Low-Cost Hyperspectral Imaging System: Design and Testing for  
1107 Laboratory-Based Environmental Applications. *Sensors (Basel)*. 20, 3293.  
1108 <https://doi.org/10.3390/s20113293>
- 1109 Suchismita, S., 2017. An analysis of barriers for plastic recycling in the Indian plastic  
1110 industry. *Benchmarking An Int. J.* 24, 415–430. [https://doi.org/10.1108/BIJ-11-2014-](https://doi.org/10.1108/BIJ-11-2014-0103)  
1111 [0103](https://doi.org/10.1108/BIJ-11-2014-0103)
- 1112 Tang, Y., Guo, Y., Sun, Q., Tang, S., Li, J., Guo, L., Duan, J., 2018. Industrial polymers  
1113 classification using laser-induced breakdown spectroscopy combined with self-  
1114 organizing maps and K-means algorithm. *Optik (Stuttg)*. 165, 179–185.  
1115 <https://doi.org/https://doi.org/10.1016/j.ijleo.2018.03.121>
- 1116 Tesfaye, W., Kitaw, D., 2020. Conceptualizing reverse logistics to plastics recycling system.  
1117 *Soc. Responsib. J.* <https://doi.org/10.1108/SRJ-12-2019-0411>
- 1118 Tsuchida, A., Kawazumi, H., Kazuyoshi, A., Yasuo, T., 2009. Identification of Shredded  
1119 Plastics in milliseconds using Raman Spectroscopy for Recycling. *Proc. IEEE Sensors*  
1120 *1473–1476.* <https://doi.org/10.1109/ICSENS.2009.5398454>
- 1121 Ulrici, A., Serranti, S., Ferrari, C., Cesare, D., Foca, G., Bonifazi, G., 2013. Efficient

- 1122 chemometric strategies for PET–PLA discrimination in recycling plants using  
1123 hyperspectral imaging. *Chemom. Intell. Lab. Syst.* 122, 31–39.  
1124 <https://doi.org/https://doi.org/10.1016/j.chemolab.2013.01.001>
- 1125 Vahid Dastjerdi, M., Mousavi, S.J., Soltanolkotabi, M., Nezarati Zadeh, A., 2018.  
1126 Identification and Sorting of PVC Polymer in Recycling Process by Laser-Induced  
1127 Breakdown Spectroscopy (LIBS) Combined with Support Vector Machine (SVM)  
1128 Model. *Iran. J. Sci. Technol. Trans. A Sci.* 42, 959–965. [https://doi.org/10.1007/s40995-](https://doi.org/10.1007/s40995-016-0084-x)  
1129 [016-0084-x](https://doi.org/10.1007/s40995-016-0084-x)
- 1130 Vázquez-Guardado, A., Money, M., McKinney, N., Chanda, D., 2015. Multi-spectral infrared  
1131 spectroscopy for robust plastic identification. *Appl. Opt.* 54, 7396–7405.  
1132 <https://doi.org/10.1364/AO.54.007396>
- 1133 Veerasingam, S., Ranjani, M., Venkatachalapathy, R., Bagaev, A., Mukhanov, V., Litvinyuk,  
1134 D., Mugilarasan, M., Gurumoorthi, K., Gunganathan, L., Aboobacker, V.M., Vethamony,  
1135 P., 2020. Contributions of Fourier transform infrared spectroscopy in microplastic  
1136 pollution research: A review. *Crit. Rev. Environ. Sci. Technol.* 1–63.  
1137 <https://doi.org/10.1080/10643389.2020.1807450>
- 1138 Wang, C., Wang, H., Fu, J., Liu, Y., 2015. Flotation separation of waste plastics for  
1139 recycling—A review. *Waste Manag.* 41, 28–38.  
1140 <https://doi.org/https://doi.org/10.1016/j.wasman.2015.03.027>
- 1141 Wang, L., 2005. Support Vector Machines: Theory and Applications, Studies in Fuzziness  
1142 and Soft Computing. Springer Berlin Heidelberg.
- 1143 Wang, X., Zhao, Y., Pourpanah, F., 2020. Recent advances in deep learning. *Int. J. Mach.*  
1144 *Learn. Cybern.* 11, 747–750. <https://doi.org/10.1007/s13042-020-01096-5>
- 1145 Wang, Z., Peng, B., Huang, Y., Sun, G., 2019. Classification for plastic bottles recycling  
1146 based on image recognition. *Waste Manag.* 88, 170–181.  
1147 <https://doi.org/https://doi.org/10.1016/j.wasman.2019.03.032>
- 1148 Wienke, D., van den Broek, W., Melssen, W., Buydens, L., Feldhoff, R., Kantimm, T., Huth-  
1149 Fehre, T., Quick, L., Winter, F., Cammann, K., 1995. Comparison of an adaptive  
1150 resonance theory based neural network (ART-2a) against other classifiers for rapid  
1151 sorting of post consumer plastics by remote near-infrared spectroscopic sensing using an

- 1152 InGaAs diode array. *Anal. Chim. Acta* 317, 1–16.  
1153 [https://doi.org/https://doi.org/10.1016/0003-2670\(95\)00406-8](https://doi.org/https://doi.org/10.1016/0003-2670(95)00406-8)
- 1154 Wu, G., Li, J., Xu, Z., 2013. Triboelectrostatic separation for granular plastic waste recycling:  
1155 A review. *Waste Manag.* 33, 585–597.  
1156 <https://doi.org/https://doi.org/10.1016/j.wasman.2012.10.014>
- 1157 Wu, X., Li, J., Yao, L., Xu, Z., 2020. Auto-sorting commonly recovered plastics from waste  
1158 household appliances and electronics using near-infrared spectroscopy. *J. Clean. Prod.*  
1159 246, 118732. <https://doi.org/https://doi.org/10.1016/j.jclepro.2019.118732>
- 1160 Yan, X., Peng, X., Qin, Y., Xu, Z., Xu, B., Li, C., Zhao, N., Li, J., Ma, Q., Zhang, Q., 2021.  
1161 Classification of plastics using laser-induced breakdown spectroscopy combined with  
1162 principal component analysis and K nearest neighbor algorithm. *Results Opt.* 4, 100093.  
1163 <https://doi.org/https://doi.org/10.1016/j.rio.2021.100093>
- 1164 Yang, Y., Zhang, X., Yin, J., Yu, X., 2020. Rapid and Nondestructive On-Site Classification  
1165 Method for Consumer-Grade Plastics Based on Portable NIR Spectrometer and Machine  
1166 Learning. *J. Spectrosc.* 2020, 6631234. <https://doi.org/10.1155/2020/6631234>
- 1167 Yu, Y., Guo, L.B., Hao, Z.Q., Li, X.Y., Shen, M., Zeng, Q.D., Li, K.H., Zeng, X.Y., Lu,  
1168 Y.F., Ren, Z., 2014. Accuracy improvement on polymer identification using laser-  
1169 induced breakdown spectroscopy with adjusting spectral weightings. *Opt. Express* 22,  
1170 3895–3901. <https://doi.org/10.1364/OE.22.003895>
- 1171 Zeng, Q., Sirven, J.-B., Gabriel, J.-C.P., Tay, C.Y., Lee, J.-M., 2021. Laser induced  
1172 breakdown spectroscopy for plastic analysis. *TrAC Trends Anal. Chem.* 140, 116280.  
1173 <https://doi.org/https://doi.org/10.1016/j.trac.2021.116280>
- 1174 Zhang, X., Lin, T., Xu, J., Luo, X., Ying, Y., 2019. DeepSpectra: An end-to-end deep  
1175 learning approach for quantitative spectral analysis. *Anal. Chim. Acta* 1058, 48–57.  
1176 <https://doi.org/https://doi.org/10.1016/j.aca.2019.01.002>
- 1177 Zhao, Q., Chen, M., 2015. Characterization of Automobile Plastics by Principal Component  
1178 Analysis and Near-Infrared Spectroscopy. *Anal. Lett.* 48, 301–307.  
1179 <https://doi.org/10.1080/00032719.2014.942910>
- 1180 Zhu, S., Chen, H., Wang, M., Guo, X., Lei, Y., Jin, G., 2019. Plastic solid waste  
1181 identification system based on near infrared spectroscopy in combination with support

1182 vector machine. *Adv. Ind. Eng. Polym. Res.* 2, 77–81.  
1183 <https://doi.org/https://doi.org/10.1016/j.aiepr.2019.04.001>  
1184